



## Million-year-scale alternation of warm-humid and semi-arid periods as a mid-latitude climate mode in the Early Jurassic (Late Sinemurian, Laurasian Seaway)

5 Thomas Munier<sup>1,2</sup>, Jean-François Deconinck<sup>1</sup>, Pierre Pellenard<sup>1</sup>, Stephen P. Hesselbo<sup>3</sup>, James B. Riding<sup>4</sup>, Clemens V. Ullmann<sup>3</sup>, Cédric Bougeault<sup>1</sup>, Mathilde Mercuzot<sup>5</sup>, Anne-Lise Santoni<sup>1</sup>, Émilie Huret<sup>6</sup>, Philippe Landrein<sup>6</sup>

<sup>1</sup> Biogéosciences, UMR 6282, uB/CNRS, Université Bourgogne Franche-Comté, 6 Boulevard Gabriel, 21000 Dijon, France.

10 <sup>2</sup> IStEP, UMR 7193, SU/CNRS, Sorbonne Université, 4 Place Jussieu, 75005 Paris, France.

<sup>3</sup> Camborne School of Mines and the Environment and Sustainability Institute, University of Exeter, Penryn Campus, Penryn, Cornwall TR10 9FE, UK.

<sup>4</sup> British Geological Survey, Keyworth, Nottingham NG12 5GG, UK.

15 <sup>5</sup> Géosciences Rennes, UMR 6118, UR/CNRS, Université Rennes 1, Campus de Beaulieu, CS 74205 35042 Rennes cedex, France.

<sup>6</sup> Agence Nationale pour la gestion des déchets radioactifs, Centre de Meuse/Haute-Marne, RD 960, 55290 Bure, France.

*Correspondence to:* Thomas Munier (thomas.munier@sorbonne-universite.fr)

**Abstract.** High resolution clay mineral and stable isotope (C, O) data are reported from the upper Sinemurian (Lower Jurassic) of the Cardigan Bay Basin (Llanbedr [Mochras Farm] borehole, northwest Wales) and the Paris Basin (Montcornet borehole, northern France) to highlight the prevailing environmental and climatic conditions. In both basins, located at similar palaeolatitudes of 30–35°N, the clay mineral assemblages comprise chlorite, illite, illite-smectite mixed-layers (R1 I-S), smectite and kaolinite in various proportions. Because the influence of burial diagenesis and authigenesis is negligible in both boreholes, the clay minerals are interpreted to be derived from the erosion of the Caledonian and Variscan massifs, including their basement and pedogenic cover. In the Cardigan Bay Basin, the variations in the proportions of smectite and kaolinite are inversely related to each other over the entire upper Sinemurian succession. As in the Pliensbachian, the stratigraphical distribution reveals an alternation of kaolinite-rich intervals reflecting strong hydrolysing conditions, and smectite-rich intervals indicating a semi-arid climate. Kaolinite is particularly abundant in the upper part of the *obtusum* Zone and in the *oxynotum* Zone, suggesting more intense hydrolysing conditions likely coeval with warm conditions responsible for an acceleration of the hydrological cycle. This interval is also marked by a negative excursion of  $\delta^{13}\text{C}_{\text{carb}}$  and  $\delta^{18}\text{O}_{\text{carb}}$ , which may confirm a warmer palaeoclimate, although these excursions may be exaggerated or overprinted by the carbonate diagenesis. In the north of the Paris Basin, the stratigraphical succession is much thinner compared to the Cardigan Bay Basin site, and the *oxynotum* Zone is either absent or highly condensed. The clay assemblages are dominantly composed of illite and kaolinite



without significant stratigraphical trends, but a smectite-rich interval identified in the *obtusum* Zone is interpreted as a  
35 consequence of the emersion of the London-Brabant Massif following a lowering of sea-level. A long-term decrease of  $\delta^{13}\text{C}_{\text{org}}$   
from the late *oxynotum*/early *raricostatum* zones is also recorded in the two sites and may precede or partly include the negative  
carbon-isotope excursion of the Sinemurian/Pliensbachian Boundary Event, recognised in most basins worldwide, and  
interpreted as a late pulse of the Central Atlantic Magmatic Province volcanism.

## 1 Introduction

40 The Early Jurassic is characterised by major palaeogeographical changes induced by the breakup of Pangaea. This geodynamic  
evolution is accompanied by intense volcanic activity corresponding to the Central Atlantic Magmatic Province (CAMP),  
beginning at the Triassic/Jurassic boundary ~201.5 million years ago (Marzoli et al., 1999; McHone, 2000; Davies et al. 2017),  
and likely responsible for the end-Triassic mass extinction (see e.g. Korte et al., 2019 and references therein). The breakup of  
45 Pangaea led to the opening of the Hispanic and Viking corridors, connecting the Tethys Ocean respectively to Panthalassa and  
the Arctic Ocean (Bjerrum et al. 2001; van de Schootbrugge et al., 2005; Damborenea et al. 2013; Porter et al., 2013). The  
disintegration of Pangaea resulted in the formation of many sedimentary basins, and palaeogeographical changes led to  
exchanges of water masses that triggered climate fluctuations with colder intervals (Dera et al., 2011) over a prolonged  
greenhouse period (Chandler et al., 1992; Dera et al., 2009a, 2015; Korte et al., 2015).

Reconstruction of seawater temperatures through the Early Jurassic are mostly deduced from  $\delta^{18}\text{O}$  measurements of belemnite  
50 rostra and some other mollusc shells, notably oysters. During the Late Sinemurian, oxygen isotope data ( $\delta^{18}\text{O}_{\text{carb}}$  and  $\delta^{18}\text{O}_{\text{belm}}$ )  
show increasing values over time (Dera et al., 2011) indicating cooler ocean temperatures, recorded for example in the  
Cleveland Basin (Hesselbo et al., 2000; Korte and Hesselbo, 2011) or the Asturian Basin (Gómez et al., 2016). However,  
warmer conditions seem to have prevailed episodically for example during the *oxynotum* Zone (Riding et al., 2013; Hesselbo  
et al. 2020).

55 The carbon cycle also shows perturbations with negative excursions, recorded either by  $\delta^{13}\text{C}_{\text{carb}}$  or  $\delta^{13}\text{C}_{\text{org}}$ . The best documented  
of these excursions is the Sinemurian-Pliensbachian Boundary Event (SPBE or S-P Event), recognised in many areas, including  
among others: the Cleveland Basin (Hesselbo et al., 2000; Jenkyns et al., 2002; Korte and Hesselbo, 2011), the Wessex Basin  
in Dorset (Jenkyns and Weedon, 2013; Price et al., 2016), the Cardigan Bay Basin in West Wales (van de Schootbrugge et al.,  
2005; Hesselbo et al., 2013; Storm et al., 2020), the Lusitanian Basin (Duarte et al., 2014; Plancq et al., 2016), the Paris Basin  
60 (Peti et al., 2017; Bougeault et al., 2017), and the Central High Atlas Basin of Morocco (Danisch et al., 2019; Mercuzot et al.,  
2019). This negative excursion is recorded in carbonates ( $\delta^{13}\text{C}_{\text{carb}}$ ), belemnite rostra ( $\delta^{13}\text{C}_{\text{belm}}$ ), and organic matter ( $\delta^{13}\text{C}_{\text{org}}$ ).  
Another  $\delta^{13}\text{C}_{\text{org}}$  negative excursion was also first recognised in the upper part of the *obtusum* Zone and through the *oxynotum*  
Zone in Eastern England (Riding et al., 2013; Hesselbo et al. 2020), and later recorded in Dorset (Southern England, Jenkyns  
and Weedon, 2013), in the Mochras borehole (Storm et al., 2020), and in the Southern Alps in Italy from shallow-water  
65 carbonate platforms to deep offshore environments (Masetti et al., 2017). This excursion coincides with increasing proportions  
of two thermophilic palynomorph taxa, *Classopollis classoides*, a terrestrially-derived pollen grain, and *Liasidium variable*,



a marine dinoflagellate cyst, suggesting that the *oxynotum* Zone was a warm and/or dry interval. *Liasidium variable*, a reliable index for the Upper Sinemurian in northwest Europe (Brittain et al., 2010; van de Schootbrugge et al., 2019), may have invaded the Tethys Ocean from Panthalassa after the opening of the Hispanic corridor (van de Schootbrugge et al., 2005). This species is particularly abundant in the *oxynotum* Zone, and the name Liasidium Event was used to describe the complex of environmental changes at this time (Hesselbo et al., 2020).

Humidity is also a key parameter of climate, but it is poorly documented over this period. Palynological data are focused on *Classopollis* pollen, which are very common in the *obtusum* and *oxynotum* zones, whether in the Cardigan Bay (Wall, 1965; van de Schootbrugge et al., 2005), the Cleveland (Riding et al., 2013) or the Lusitanian basins (Poças Ribiero et al., 2013).

The composition of clay mineral assemblages can be a reliable climate indicator (Chamley, 1989; Ruffell et al., 2002; Raucsik and Varga, 2008; Dera et al., 2009b) provided their dominant detrital origin can be demonstrated. Clay mineral assemblages may reflect the intensity of hydrolysis during pedogenic processes and runoff conditions on landmasses, and thus specify humidity variations from the signal recorded in marine sedimentary series. In the Upper Sinemurian, variations of clay mineral assemblages have been studied on several outcrops and boreholes from the British Isles (Jeans, 2006; Kemp et al. 2005; Hesselbo et al., 2020) and in the Montcornet borehole, north of the Paris Basin (Debrabant et al., 1992), but at low resolution, only for a short interval, or in successions affected by strong clay mineral diagenesis. Here we attempt, through a high-resolution study of detrital clay mineral assemblages and fluctuations in stable isotopes (C and O) of Upper Sinemurian strata from the Llanbedr (Mochras Farm) and the Montcornet boreholes, to estimate the intensity of chemical weathering, of hydrolysis, and the magnitude of carbon cycle changes.

## 2 Geological background

During the Early Jurassic, the Paris and Cardigan Bay basins were located to the north west of the Tethyan domain. This area corresponded to an archipelago of large islands inherited from Caledonian and Variscan massifs (Thierry et al., 2000). These continental masses, such as the London-Brabant Massif, the Massif Central and Armorican Massif, and the Welsh High, were surrounded by an epicontinental sea (Fig. 1). An excellent sedimentary record of the Early Jurassic is preserved at both study locations due to the extensional context linked to the breakup of Pangaea and related thermal and tectonic subsidence (Woodland et al., 1971; Corcoran and Clayton, 1999; Guillocheau et al., 2000; Beccaletto et al., 2011; Hesselbo et al., 2013).

### 2.1 The Llanbedr (Mochras Farm) borehole, Cardigan Bay Basin, Wales

The Cardigan Bay Basin, located in West Wales, between the Welsh High and the Irish Massif (Fig. 1), corresponds to a half-graben basin (Dobson and Whittington, 1987; Tappin et al., 1994; Holford et al., 2005), bounded at the end of the Palaeozoic by a major active fault (the Mochras Fault) with an offset of almost 4500 m (Wood and Woodland, 1968; Woodland, 1971, Hesselbo et al., 2013). This basin was located at a latitude between 35°N and 40°N (Fig. 1; Thierry et al., 2000). Lower Jurassic strata reach ~1300 m in thickness (Woodland et al., 1971; Ruhl et al., 2016), and contrast with overlying thinner Middle and



Upper Jurassic successions (Dobson and Whittington, 1987). Cretaceous strata are rare or absent, because of erosion following thermal uplift and inversion processes (Woodland et al., 1971; Tucker and Arter, 1987; Tappin et al., 1994), while the thickness of Cenozoic sedimentary rocks reaches 600 m.

The Llanbedr (Mochras Farm) borehole, commonly abbreviated to Mochras, was drilled between 1967 and 1969 on the coast in northwest Wales, UK (Fig. 2) (Woodland et al., 1971; Hesselbo et al., 2013). The Lower Jurassic deposits consist of a continuous succession of marls and claystones, making this borehole a reference for environmental and climatic reconstructions for the Early Jurassic (Hesselbo et al., 2013).

The 220 m-thick Upper Sinemurian strata consist of relatively homogeneous marls and clayey mudstones, with more silt in the upper part of the *raricostatum* Zone. Veins of calcite and pyrite commonly occur and siderite nodules are present, particularly in the *oxynotum* Zone. It has previously been suggested that this calcite veined level may have been the consequence of faulting leading to very minor stratigraphical offset according to biostratigraphical data (Woodland et al., 1971; Storm et al., 2020), but there is no positive evidence for strata missing due to tectonism.

Following the zonation proposed by Page (2003), a precise biostratigraphical scheme is established, based on the frequent occurrence of ammonites (Hesselbo et al., 2013; Page in Copestake and Johnson, 2014). The *obtusum* Zone extends from 1468 to 1376 m, overlain by the *oxynotum* Zone to 1332 m, and the *raricostatum* Zone from 1332 to 1249 m (Woodland et al., 1971).

## 2.2 Montcornet borehole, Paris Basin, France

During the Early Jurassic, the Paris Basin was bordered by continental masses, remnants of the Palaeozoic orogenic belts (Fig. 1). The main landmasses include the London-Brabant Massif (LBM), the Armorican Massif, the Massif Central, and the Bohemian Massif (Guillocheau et al., 2000; Thierry et al., 2000).

The Montcornet borehole (borehole Andra A901) was drilled in 1989 near the village of Montcornet to the north of the Paris Basin (Fig. 3), by Andra, the French National Radioactive Waste Management agency. The strata penetrated were deposited in an epicontinental sea located immediately south of the LBM, at a palaeolatitude of approximately 35°N, quite similar to the latitude of the Cardigan Bay Basin (Fig. 1). The stratigraphical succession extends from the Devonian metamorphic basement (shales) to the Turonian chalk, with a major gap occurring for the Lower Cretaceous, corresponding to the continental evolution of the Paris Basin (Wealden facies), from the Purbeckian deposits to the upper Albian transgressive claystones and marls (Debrabant et al., 1992). Above the siliciclastic continental Triassic deposits, at a depth of ~1075 m, Jurassic strata, nearly 870 m thick, correspond mainly to open-marine limestones and marls (Yang et al., 1996).

The Upper Sinemurian succession (~50 m, Fig. 4) consists of alternations of claystone, marl and bioclastic limestone beds characterised by the presence of bivalves (*Gryphaea*), likely deposited in lower to upper offshore environments according to Yang et al. (1996).

The biostratigraphical calibration is complicated by the occurrence of some important hiatuses and by the relative scarcity of ammonites. Some new determinations (by J.L. Dommergues) on ammonites found during the sampling complete the previous



biostratigraphical scheme of Yang et al. (1996) and are illustrated in Fig. 4. Ammonites from the *semicostatum* Zone (Lower Sinemurian) are identified up to 976 m while the first ammonite from the *obtusum* Zone occurs at 948.88 m with *Promicroceras* gr. *planicosta* (Yang et al., 1996, Fig. 4). The *turneri* Zone is not identified, but may be present between 976 m and 948.88 m. However, the occurrence of the dinoflagellate *Liasidium variabile* in this interval strongly suggests a Late Sinemurian age, the  
135 miss of the *turneri* Zone (Fauconnier, 1995; Bucefalo Palliani and Riding, 2000) and that the *obtusum* Zone starts at 976 m. The last ammonite of the *obtusum* Zone is identified at 939.80 m while the first ammonite of the *raricostatum* Zone is identified at 937.82 m (Yang et al., 1996) or slightly lower (938.55 m) according to new determinations of *Crucilobicerias* sp. that would indicate the *densinodulum* Subzone of the *raricostatum* Zone. (Fig. 4). No ammonites from the upper part of the *obtusum* Zone or from the *oxynotum* Zone have been found. This interval is, as is the case in the Wessex Basin in Dorset (Lang, 1945; Hallam  
140 1999; Hesselbo, 2008) and the Lower Saxony Basin of Germany (van de Schootbrugge et al., 2019), either absent or highly condensed in a 1.25 m thick interval without any ammonites between 939.80 and 938.55 m. The last ammonites of the *raricostatum* Zone are identified up to 921.75 m, in agreement with the occurrence of *Liasidium variabile* up to 922 m (Fauconnier, 1995), while the first ammonites of the *jamesoni* Zone appear from 920.6 m, suggesting that the Sinemurian/Pliensbachian boundary is located at ~921 m (Fig. 4). However there are also some gaps at the  
145 Sinemurian/Pliensbachian transition since the upper part of the *raricostatum* Zone (*aplanatum* Subzone) is possibly missing, and since the base of the *jamesoni* Zone (*taylori* Subzone) is also missing.

### 3 Material and methods

#### 3.1 Clay mineral analyses

A total of 223 samples were analysed using X-Ray Diffraction (XRD). After moderate grinding in a mortar, powdered samples  
150 were decarbonated with a 0.2N HCl solution. The < 2 µm fraction (clay-sized particles) was extracted with a syringe after decantation of the suspension for 95 minutes following Stokes' Law; this fraction was then centrifuged. Clay residue was then smeared on oriented glass slides and run in a Bruker D4 Endeavor diffractometer with CuK<sub>α</sub> radiation, a LynxEye detector and a Ni filter with a voltage of 40 kV and an intensity of 25 mA (Biogéosciences laboratory, University of Burgundy, France). Goniometer scanning ranged from 2.5° to 28° for each analysis. Three runs were performed for each sample to discriminate  
155 the clay phases: 1) air-drying; 2) ethylene-glycol solvation; and 3) heating at 490°C for two hours, as recommended by Moore and Reynolds (1997). Clay minerals were identified using their main diffraction (*d*<sub>001</sub>) peaks and by comparing the three diffractograms obtained. The following main clay minerals were identified: a R0 type illite-smectite mixed-layer (17 Å based on a glycolated run) referred to as smectite for the following sections; a R1 type illite-smectite mixed-layer (around 11.5 Å in air-drying conditions and 13 Å after ethylene-glycol solvation); chlorite (14.2 Å, 7.1 Å, 4.7 Å and 3.54 Å peaks); illite (10 Å,  
160 5 Å, 3.33 Å peaks) and kaolinite (7.18 Å and 3.58 Å peaks). Each clay mineral was quantified using the MacDiff software (version 4.2.5) (Petschick, 2001) on glycolated sample diffractograms. The area of main peaks (*d*<sub>001</sub>) is measured to estimate by semi-quantification, the proportion of each clay species. As the main (*d*<sub>001</sub>) peak of kaolinite and the (*d*<sub>002</sub>) peak of chlorite



165 overlap, a deconvolution procedure was applied on the ( $d_{004}$ ) peak area of chlorite (3.54 Å) and ( $d_{002}$ ) peak area of kaolinite (3.57 Å) to accurately quantify both mineral portions using the 7.1 peak ( $d_{001\text{kaolinite}} + d_{002\text{chlorite}}$ ). Chlorite percentage was calculated using the mean between ( $d_{001}$ ) and ( $d_{002}$ ) chlorite peak areas considering that the chemical nature of chlorite impacts the ( $d_{001}$ )/( $d_{002}$ ) ratio (Moore and Reynolds, 1997). The error margin of this method is approximately  $\pm 5\%$  on the relative proportions of clay minerals in the clay fraction. The relative proportions of clay minerals are estimated using the ratios between the areas of the peaks, the most relevant of these being the K/I and Sm/K ratios.

### 3.2 Geochemical preparation and analyses

170 Seventy samples from the Mochras borehole and 38 samples from the Montcornet borehole were selected for  $\delta^{13}\text{C}_{\text{org}}$  analyses. One gram of sample, previously crushed, underwent an acid digestion by 10 ml of 6N HCl solution for 48 hours, a concentration and a duration justified by the common occurrence of dolomite. After cleaning with pure water, decarbonated powders were dried in an oven (50°C for 24 to 48 hours), then crushed again to obtain a fine powder. Each sample, of a specific mass (9 to 75 mg, depending on former sample  $\text{CaCO}_3$  content), is weighed in a tin capsule with a Sartorius M2P ultrabalance.

175 Samples were analysed with the Elementar MICRO cube elemental analyser coupled to an Elementar Isoprime 100 isotope ratio mass spectrometer. Isotope ratios obtained were compared to international standards USGS40 L-glutamic acid ( $\delta^{13}\text{C} = -26.39 \pm 0.04\%$  V-PDB) and IAEA-600 caffeine ( $\delta^{13}\text{C} = -27.77 \pm 0.04\%$  V-PDB). For each sample, replicates showed reproducibility better than  $\pm 0.15\%$ . The total organic carbon (TOC) content, expressed in wt.% was determined by the elemental analyser at the same time.

180 Bulk rock carbon and oxygen isotope ratios analyses coupled with  $\text{CaCO}_3$  concentration measurements were carried out using a Sercon 20-22 triple detector Gas Source Isotope Ratio Mass Spectrometer at the University of Exeter Penryn Campus following methods described in detail in Ullmann et al. (2020). Bulk rock powder extracted from rock fragments with a handheld drill was weighed at 1 µg precision and transferred into borosilicate vials targeting an amount of 500 µg of  $\text{CaCO}_3$  for analysis. Samples were flushed with He to remove atmospheric gases and then reacted with nominally anhydrous phosphoric acid (“103 %”) at 70°C. In a single batch 80 samples were analysed together with two in-house standards (22 aliquots of CAR- Carrara Marble,  $\delta^{13}\text{C} = +2.10\%$  V-PDB;  $\delta^{18}\text{O} = -2.03\%$  V-PDB; 8 aliquots of NCA- Namibia Carbonatite,  $\delta^{13}\text{C} = -5.63\%$  V-PDB;  $\delta^{18}\text{O} = -21.90\%$  V-PDB). Instrumental drift and biases were corrected using a two-point calibration constrained by these two in-house standards. Accuracy was ensured via previous calibration of the in-house standards against international certified standards.  $\text{CaCO}_3$  content was computed from matching signal intensity of unknowns with CAR, which

190 is assumed to be 100% pure  $\text{CaCO}_3$  (44 wt%  $\text{CO}_2$ ). Reproducibility of the isotope ratio measurements for Mochras bulk rock samples based on analyses of CAR (2 s.d.,  $n = 300$ ) is 0.07 ‰ for  $\delta^{13}\text{C}$  and 0.16 ‰ for  $\delta^{18}\text{O}$ . Reproducibility of  $\text{CaCO}_3$  determinations are based on multiple analysis of NCA as an unknown which gave  $97.2 \pm 1.3\%$  (2 s.d.,  $n = 132$ ).  $\text{CaCO}_3$  content was measured using a Bernard calcimeter (volumetric calcimetry) on samples, completed by weight-loss method (weight difference between the sample before and after decarbonation was performed prior to isotopic analyses on



195 organic matter) for each sample. Each curve obtained for the geochemical data has been refined as a smoothed curve and its  
95% confidence intervals acquired from a Kernel type regression using different levels of smoothing for each borehole.

## 4 Results

### 4.1 CaCO<sub>3</sub> and Total Organic Carbon (TOC) contents

Calcite content from the Upper Sinemurian of the Mochras borehole shows substantial fluctuations between 3 and 62% (Fig.  
200 5). The Lower Sinemurian/Upper Sinemurian boundary is relatively rich in carbonate, up to 40%, but the lowermost and the  
uppermost parts of the *obtusum* Zone are depleted in CaCO<sub>3</sub> (<10%), while in the middle part of this ammonite zone the CaCO<sub>3</sub>  
content ranges from 20 to 40%. The low CaCO<sub>3</sub> content recorded at the top of the *obtusum* Zone persists in the lower half of  
the *oxynotum* Zone. Then, in the upper half of this zone and in the *raricostatum* Zone, CaCO<sub>3</sub> increases up to 60% (Fig. 5). In  
the Montcornet borehole CaCO<sub>3</sub> content also fluctuates between 3 and 62%, with similar trends, notably: 1) a depletion in the  
205 uppermost part of the *obtusum* Zone, although less well expressed than in the Mochras borehole likely because of the  
condensation of the series, and; 2) a significant increase in the *raricostatum* Zone (Fig. 6).

Total organic carbon (TOC) measurements are also similar between the two boreholes with proportions around 1% (Figs 7,  
8). The Lower Sinemurian/Upper Sinemurian boundary is marked by a slightly higher TOC content (1.5%) while the top of  
the *obtusum* Zone shows a decrease in the proportion of organic carbon (0.5%). In the Mochras borehole, the *macdonnelli-*  
210 *aplanatum* subzones of the *raricostatum* Zone are enriched in TOC with values generally higher than 1.5% and reaching 3%.

### 4.2 Clay mineralogy

#### 4.2.1 Mochras borehole

Upper Sinemurian clay mineral assemblages are dominantly composed of chlorite (5 to 32%), illite (15 to 42%), R0 type  
illite/smectite mixed-layers hereafter called smectite (10 to 60%) and kaolinite (4 to 32%). Minor proportions of R1 type  
215 illite/smectite mixed-layers are commonly associated with these minerals. Significant fluctuations in the relative proportions  
of the different clay species are recorded along the core. The main striking feature is the inverse relationship between smectite  
and kaolinite, particularly well-expressed by the Sm/K ratio (Fig. 5). The opposition of these two minerals determines an  
alternation of kaolinite-rich packages of sediments (lower part of *obtusum*, top of *obtusum*/base *oxynotum* and median part of  
*raricostatum*), and of smectite-rich packages of sediments (middle part of *obtusum*, upper part of the *oxynotum* zone / base  
220 *raricostatum*, and upper part of *raricostatum*).

The proportions of chlorite are relatively high and fluctuate in parallel with those of kaolinite. From the base to the top of the  
Upper Sinemurian, the proportion of illite increases more or less regularly from ~20 to 40%.



#### 4.2.2 Montcornet borehole

The clay mineral assemblages of the Upper Sinemurian of the Montcornet borehole are composed of the same minerals as the Mochras borehole, but show much less variation (Fig. 6). Illite is the most abundant clay mineral with proportions from 25 to 46%, without any clear trend through the core. Kaolinite is also abundant with proportions ranging from 6 to 32%, most samples having values close to 22%. Chlorite shows lower percentages, between 9 and 24% (average of ~19%). According to Debrabant et al. (1992), this mineral is associated with small proportions of chlorite/smectite mixed-layers, undifferentiated on Fig. 6. R1 type illite/smectite mixed layers are relatively abundant between 5 to 26% notably in the middle part of the *obtusum* Zone. Smectites are absent over a large part of the 56 m of Upper Sinemurian, but these clay minerals occur in significant proportions (up to 33%) in an eight metre-thick interval between 965 and 973 m within the *obtusum* Zone (Fig. 6).

### 4.3 Carbon and oxygen isotope fluctuations

#### 4.3.1 Mochras borehole

Organic carbon isotopes ( $\delta^{13}\text{C}_{\text{org}}$ ) values show significant variations (about 3.9‰) between -24.47 and -28.34‰ over the Upper Sinemurian succession (Fig. 7).  $\delta^{13}\text{C}_{\text{org}}$  values show little variations in the *obtusum* and *oxynotum* zones (around -25/-26‰), while in the *raricostatum* Zone, an irregular decrease of the values down to -28‰ is recorded.

$\delta^{13}\text{C}_{\text{carb}}$  shows significant variations of more than 5‰ with values between +3.04 and -2.21‰ V-PDB (Fig. 7). A prominent negative excursion (~ 3‰) is recorded at the transition between the *obtusum* and the *oxynotum* Zones followed by an increasing trend up to the topmost part of the Sinemurian. A slight negative excursion (1‰) is recorded at the transition between the *densinodulum/raricostatum* and *macdonnelli/aplanatum* subzones (Fig. 7).

$\delta^{18}\text{O}_{\text{carb}}$  values range from -6.54 to -2.61‰ (Fig. 7). Very large fluctuations are recorded in the *obtusum* and *oxynotum* zones, while more constant values around -4‰ are observed in the *raricostatum* Zone. The major part of the *oxynotum* Zone corresponds to an interval characterised by lower values.

#### 4.3.2 Montcornet borehole

The isotope data ( $\delta^{13}\text{C}_{\text{org}}$ ) from the Montcornet borehole show values between -26.49 and -24.66‰ (Fig.8). The trends are similar to those of the Mochras borehole, although less well-expressed likely due to the condensation of the series and the probable occurrence of hiatuses. The values increase slightly from the base of the core to the transition between the *obtusum* and *raricostatum* zones, while a decreasing trend is observed in the *raricostatum* Zone to the base of the Pliensbachian. The isotopically lowest values of ~-26.5 ‰ recorded in the *raricostatum* Zone are however higher than at Mochras.





## 5 Discussion

### 5.1 Diagenetic influence

#### 5.1.1 Influence of diagenesis on clay mineral assemblages

The use of clay minerals as climatic proxies assumes that these minerals are mainly of detrital origin. However, the increase in temperature associated with burial may trigger various transformations of detrital clay minerals to change the constitution of detrital clay assemblages. In fine-grained clayey and marly sediments, among the possible transformations, the illitisation of smectite is certainly the most important. The illitisation of smectites into R1-type illite/smectite mixed-layers begins when the temperatures reach 60-70° C at a depth of burial of the order of 2000 m, considering a normal geothermal gradient (Šucha et al., 1993; Lanson et al., 2009; Dellisanti et al., 2010).

The occurrence of abundant smectite in the Sinemurian strata in the Mochras borehole and the presence of a smectite-rich interval in the Montcornet borehole indicate a limited diagenetic influence due to the relatively shallow depth of burial. In both boreholes, the maximum burial temperatures probably never exceeded 70°C, which is consistent with the geological history of the Cardigan Bay and Paris basins. In the Cardigan Bay Basin, the thickness of the sediments overlying the Sinemurian can be estimated to be ~1400 m including 800 m of Lower Jurassic and ca. 600 m of Oligo-Miocene and Quaternary sedimentary rocks, with, of course, any of the younger Mesozoic strata eroded before deposition of the Cenozoic sediments (Tappin et al., 1994; Holford, 2005). The negligible influence of burial diagenesis is also confirmed by the occurrence of immature to only marginally mature organic matter (OM) revealed by Rock Eval pyrolysis data from the Sinemurian mudrocks (van de Schootbrugge et al., 2005; Storm et al. 2020). In the Sinemurian succession,  $T_{\max}$  values range between 423 and 436°C (average 428°C,  $n = 195$ , Storm et al., 2020) indicated immature OM or occasionally early mature OM at the onset of the oil window.

Vitrinite reflectance ( $R_0$  max) data suggest a higher maximal burial temperature of the Sinemurian strata (Corcoran and Clayton, 1999) ranging between 83 and 90°C (Holford et al., 2005), but these authors discarded the lowest values of  $R_0$  (low burial temperatures), considering that these data were not reliable enough. Such high temperatures are incompatible with both the occurrence of smectite and with the presence of immature organic matter, and therefore we consider that the low values of vitrinite reflectance data published by Holford et al. (2005) are fully realistic.

In the Montcornet borehole, the depth of burial of the Upper Sinemurian can be estimated at a maximum of ca. 2000 m, including the entire Jurassic succession (870 m), ca. 200 m of Cenomanian and Turonian chalks and now eroded/dissolved Coniacian to Maastrichtian chalks. The Coniacian to Campanian chalk is ~ 400 m-thick in central Paris Basin (southwest of Paris, Robaszynski et al., 2005) but the uppermost Campanian and Maastrichtian deposits were eroded and therefore the thickness of the entire Upper Cretaceous is difficult to estimate. To the East of the Paris Basin, a maximum thickness of the chalk deposits is estimated around only 200 m (Blaise et al., 2014). According to the apatite fission-track thermochronology study of Barbarand et al. (2018), the entire Cretaceous deposits would have a thickness of 1000 m, which seems to be a maximum value. Assuming a total burial depth of 2000 m, which represents probably a maximum, the burial-temperature rise probably did not exceed 60°C, which is consistent with the preservation of smectite. This is also confirmed by  $T_{\max}$  data which



range between 423 and 426°C in the Sinemurian of the Montcornet borehole, indicating that organic matter is still immature  
285 (Disnar et al., 1996; Mercuzot et al., 2019).

Clay diagenesis can be also revealed by relationships between clay mineralogy and the lithology, notably in marl-limestone  
alternations (Deconinck and Debrabant, 1985; Deconinck, 1987; Levert and Ferry, 1988), but in the two studied boreholes,  
there is no statistically strong correlation between CaCO<sub>3</sub> content and the proportion of each clay species (Fig. 9). As an  
example, in the Mochras borehole, the proportion of smectite is weakly correlated with the percentages of CaCO<sub>3</sub> ( $r=0.31$ ,  $n$   
290  $= 128$ ,  $p$ -value  $< 0,05$ ) which likely indicates that a possible better preservation of smectite on carbonate-rich interval can be  
excluded.

The occurrence of authigenic well-crystallised kaolinite can also be envisaged, as it was previously observed in some porous  
carbonates in the upper Pliensbachian of the Paris Basin (e.g. Bougeault et al., 2017). However, this phase can be easily  
highlighted on diffractograms by the presence of very narrow peaks indicating a good crystallinity, which is not the case here,  
295 thus excluding the occurrence of measurable authigenic kaolinite. Moreover, sampling of porous limestones has been avoided.  
Contrary to what has been observed in the overlying Pliensbachian strata of the Mochras borehole, we do not identify any  
authigenic mineral such as clinoptilolite or berthierine whose presence there in small quantities is likely in the Pliensbachian  
(Deconinck et al., 2019). Consequently, we infer that most clay minerals identified in the Sinemurian of the two studied  
boreholes are dominantly detrital and carry climatic and environmental information.

300

### 5.1.2 Impact of diagenesis on isotopic data

Fluid circulations and temperature may disturb the primary isotope signal in sediment during late diagenesis, notably for the  
bulk carbonate signal (Anderson, 1969; Hudson, 1977; Marshall, 1992). Early diagenesis may also impact the isotope signal  
from bulk carbonate when low calcium carbonate content is present (Ader and Javoy, 1998; Bougeault et al., 2017).  
305  $\delta^{18}\text{O}$  values are more sensitive to fluid circulation and recrystallisation, particularly in porous rocks, normally leading to more  
negative and/or scattered values (Hudson, 1977; Marshall, 1992; Stoll and Schrag, 2000). Although the low porosity and  
permeability of clayey limestones, marls and claystones of the Mochras and Montcornet boreholes are not favourable to fluid  
circulation, some diagenetic features such as the occurrence of nodular beds, and calcite and siderite nodules, suggest that  
isotopic values may be significantly altered by diagenetic processes. In the Montcornet borehole, this is the case in the  
310 underlying Hettangian succession where the secondary crystallisation of calcite in sulphate-reducing environments is  
responsible for a depletion in <sup>13</sup>C (Ader and Javoy, 1998). In the overlying Pliensbachian strata of this borehole, an alteration  
of the  $\delta^{13}\text{C}_{\text{carb}}$  was observed by Bougeault et al. (2017), notably in a carbonate-depleted interval ( $<10\%$  CaCO<sub>3</sub>) with common  
siderite and calcite nodules, suggesting a migration of carbonate within clayey series. An interval with similar characteristics  
(clay-rich strata with common carbonate concretions, traces of siderite) is present in the *obtusum/oxynotum* zone transition in  
315 the Mochras borehole (Woodland et al., 1971). The significant correlation ( $r = 0.68$ ,  $n = 96$ ,  $p$ -value  $< 0,05$ ) between the  
carbonate content and the  $\delta^{13}\text{C}_{\text{carb}}$  values could reflect the disturbance of the inorganic carbon signal in a clayey interval more



sensitive to diagenesis. A disturbance of the isotopic signal of carbon and oxygen from carbonates in this more clayey interval is likely especially when measurements taken on the carbon of organic matter and microfossils do not show parallel variations (Ullmann unpublished data).

320 Long distance correlations can be made based on the comparison of  $\delta^{13}\text{C}_{\text{org}}$  fluctuations through the Lower Jurassic in several sedimentary basins, likely reflecting a primary signal (Storm et al., 2020), even if diagenetic impacts on organic compounds may locally be significant (Meyers, 1994; Lehmann et al., 2002). Consequently, in the case of the Mochras and Montcornet boreholes, the  $\delta^{13}\text{C}_{\text{org}}$  seems to be much more reliable to constrain carbon-cycle perturbations during the Late Sinemurian, while  $\delta^{13}\text{C}_{\text{carb}}$  and  $\delta^{18}\text{O}$  values cannot be interpreted confidently in terms of environmental and climatic fluctuations.

## 325 **5.2 Environmental significance of clay mineral assemblages**

### **5.2.1 Detrital sources of clay minerals**

Although clay minerals may be transported over long distances, the Welsh High and the Irish Massif were likely the main detrital sources of the Cardigan Bay Basin (Dobson and Whittington, 1987; Xu et al. 2018). In the coeval deposits of the Dorset coast, southern England, the clay assemblages show a similar composition, but smectite is less abundant, suggesting that  
330 detrital inputs into the Wessex Basin originated from distinct detrital sources including the Cornubian and the Armorican massifs (Schöllhorn et al., 2020a). In the Paris Basin, the main detrital sources of clay minerals were probably the proximal Palaeozoic massifs, including the London-Brabant Massif (LBM), the Armorican Massif and the Massif Central (Muller et al., 1973; Debrabant et al., 1992; Thierry et al., 2000), as suggested by dominant continental organic matter preserved in the Jurassic sediments drilled at Montcornet (Disnar et al., 1996).

335 The abundance of illite and chlorite reflects the intensity of erosion of these continental areas. Precambrian and/or Palaeozoic mudrocks from the Welsh High and from the LBM mainly contain mica-illite, chlorite, and corrensite (regular chlorite/smectite mixed-layer) reflecting deep burial and low-grade metamorphism (Lefrançois et al., 1993; Han et al., 2000; Merriman, 2006; Hillier et al., 2006). These assemblages occur in most Variscan massifs in Europe, and as a result, the high proportions of chlorite and illite in most Jurassic sedimentary successions of northwest Europe reflects mostly the erosion of these Palaeozoic  
340 and older rocks (Jeans et al., 2001). In the Mochras borehole, from the base to the top of the Upper Sinemurian, the proportions of illite increase from ca. 20 to 35%. This evolution suggests that during the Late Sinemurian, an increasing erosion of the Welsh High basement occurred, compared to the development of thick soils. This may be the consequence of a long-term uplift of the Welsh High aided by faulting. By comparison, the constant proportions of illite recorded in the Montcornet borehole, located proximately south of the LBM, suggest continuous unchanged processes of erosion on this tectonically stable  
345 massif.

In sediments, smectites have various origins. These minerals are most often reworked from soils where they formed under warm and seasonally humid climate (Chamley, 1989). But smectite can also be formed in marine environments either at the expense of volcanic glass or as an authigenic phase in slowly deposited sediment (Deconinck and Chamley, 1995). The



350 Sinemurian strata from the Mochras borehole do not show any evidence of volcanic origin and were rapidly deposited, with high sedimentation rates responsible for their particularly high thickness (220 m for the Upper Sinemurian). The duration of the Upper Sinemurian is estimated at 3 Myr, which suggests an average sedimentation rate (after compaction) of more than 70 m/Myr (Storm et al., 2020). In the *macdonnelli-aplanatum* subzones, a high mean sedimentation rate of ca. 40 m/Myr can be estimated considering a duration of about 800 kyr of these subzones, according to cyclostratigraphical studies (Ruhl et al., 2016). These relatively high sedimentation rates are not favourable to smectite authigenesis and consequently, most smectite  
355 minerals identified here are likely detrital and originated from pedogenic blankets developed over the Welsh or Irish massifs during periods of warm and seasonally humid climate.

Kaolinite, as for illite or chlorite, can be reworked from kaolinite-bearing sedimentary rocks and from the palaeoweathering profile in continental areas (Hurst, 1985). Kaolinite may be reworked from sandstones where its authigenic formation is common as pore filling booklets, such as Devonian (Old Red Sandstone) and Carboniferous sandstones from southern England  
360 and Wales (Hillier et al., 2006; Shaw, 2006; Spears, 2006). Kaolinite may also originate from soils formed under hot and regularly humid climate (Chamley, 1989; Ruffell et al., 2002). In both cases, increasing proportions of kaolinite in a sedimentary succession suggest enhanced runoff favoring erosional processes and/or hydrolysing climate.

### 5.2.2 Environmental control of the clay sedimentation

In the Mochras borehole, the clay mineralogy of the Upper Sinemurian is relatively similar to that observed in the overlying  
365 Pliensbachian formations, where an antagonistic evolution in the relative proportions of smectite and kaolinite is recorded. The alternation of kaolinite-rich and smectite-rich intervals was interpreted for the Pliensbachian to be the result of climate fluctuations, respectively dominated by regularly humid periods and semi-arid conditions (Deconinck et al., 2019). This climate mode seems to be established at least at the beginning of the Late Sinemurian on the Welsh High and the surrounding massifs. In the northern Paris Basin, in the Montcornet borehole, such climatic fluctuations are not recorded, even though this  
370 basin was located at a comparable palaeolatitude as the Cardigan Bay Basin. Apart from the smectite-rich interval occurring at the transition between the Lower and the Upper Sinemurian and at the base of the *obtusum* Zone, the clay mineralogy is rather uniform. In this borehole, such smectite-rich intervals referred as “smectite events” were also recorded in the Pliensbachian sediments (Bougeault et al., 2017). The occurrence of these “smectite events” was interpreted as the result of the lowering of the sea-level favouring the formation of smectite in soils developed on newly exposed lands of the LBM. The  
375 Lower/Upper Sinemurian boundary and the base of the *obtusum* Zone are precisely characterised by relative sea-level lowstands in the northwest European domain (Jacquin et al., 1998; Hesselbo 2008; Haq, 2018). Therefore, the smectite-rich interval occurring in the Sinemurian of Montcornet is also interpreted as a consequence of the lowering of the sea level allowing the formation of smectite on newly exposed lands of the LBM with its comparatively subdued relief. By contrast, during relative sea-level highstand, the LBM was probably at least partly flooded, suggesting that this massif was already deeply  
380 eroded and relatively flat as early as the Sinemurian. A similar behaviour of this massif regarding sea-level fluctuations lasted until the Late Jurassic (Hesselbo et al., 2009). Consequently, the LBM being often submerged, it is probable that the clay



minerals deposited to the south of this massif had partly a more distant origin, and this may explain the difference with the Cardigan Bay Basin. The sea-level highstand during the *oxynotum* Zone is likely responsible for the starvation of the Paris Basin, with a reduced sedimentation rate and even the significant sedimentary gap equally observed on the Dorset coast (cf. Hallam 1999, 2000; Coe and Hesselbo 2000; Hesselbo et al., 2020).

### 5.2.3 Kaolinite-rich intervals- Mochras borehole

The three kaolinite-rich intervals observed in the Mochras borehole are highlighted by the kaolinite/illite and smectite/kaolinite ratios (respectively K/I and Sm/K Fig.10). These intervals occur: (1) at the base of the *obtusum* Zone (interval K1), (2) around the boundary between the *obtusum* and *oxynotum* zones (interval K2), and (3) in the *raricostatum* Zone (interval K3). The onset of a fourth kaolinite-rich interval is present at the Sinemurian/Pliensbachian boundary and lasted through to the lower part of the *jamesoni* Zone (Deconinck et al., 2019).

These intervals may be associated with more humid conditions, but in detail, they occur in different tectonic and eustatic settings. K1 occurs during a period of lowstand of the sea-level (Hesselbo, 2008). These conditions may have enhanced the proportions of kaolinite since this mineral is well-known to be deposited preferentially in proximal environments due to differential settling processes of clay minerals (Gibbs, 1977; Godet et al., 2008). Therefore, we suggest that the high proportions of kaolinite could be the result of combined influences of a more humid climate and relative low sea-level conditions. By contrast, K2 occurs during a period of a high sea level, favourable to the deposition of more smectite. Consequently, as this kaolinite-rich interval is also the most prominent, it is probable that the climatic conditions were particularly hydrolysing (wet and/or warm) from the upper part of the *obtusum* zone to the lower part of the *oxynotum* Zone. The resulting significant detrital fluxes were probably responsible for a dilution of the carbonates, leading to a more clay-rich sedimentation during this interval. The proportions of kaolinite in K3 are lower than in K1 and K2 and this interval is also marked by the relative abundance of illite, suggesting more efficient erosion of the basement that may be linked to tectonic influences. It is therefore possible that in K3, kaolinite may be partly reworked together with illite from the unmetamorphosed rocks of the basement.

Interestingly, the three kaolinite-rich intervals seem to coincide with higher values of  $^{87}\text{Sr}/^{86}\text{Sr}$  ratio consistent with increasing detrital influences linked to the acceleration of the hydrological cycle (Fig. 10). The most prominent increase of  $^{87}\text{Sr}/^{86}\text{Sr}$  ratio precisely coincides with the most prominent increase of kaolinite (K2) that occurs around the transition between the *obtusum* and the *oxynotum* Zones. It should be noted, however, that the fluctuations in  $^{87}\text{Sr}/^{86}\text{Sr}$  ratio correspond to a global signal while the clay minerals register a local signal.

To summarise, the three kaolinite-rich intervals are indicative of increasing moisture. Of these, K2 occurring during the uppermost part of the *obtusum* Zone and the lower part of the *oxynotum* Zone is of particular interest, as it is at least indicative of a significant acceleration of the hydrological cycle. This interval is also characterised by low  $\delta^{18}\text{O}$  values consistent with warm conditions, but these low values may also reflect enhanced freshwater inputs as a consequence of increasing runoff (Fig. 7; Deconinck et al., 2019; Schöllhorn et al., 2020a;). In addition, these  $\delta^{18}\text{O}$  values are likely to have been affected by diagenetic



415 influences (section V.1.2) and therefore cannot be held here as a reliable proxy of seawater temperature. In the Copper Hill  
borehole drilled close to Ancaster in Lincolnshire, East England this interval is characterised by the abundance of *Classopollis*  
also indicating warm climate and by a negative excursion of -2/-3 ‰ of  $\delta^{13}\text{C}_{\text{org}}$  (Riding et al., 2013). Surprisingly, this negative  
excursion is less clearly recorded in organic carbon at Mochras (Fig.10; van de Schootbrugge et al., 2008; Storm et al., 2020).

### 5.3 Carbon cycle evolution and SBPE record

420 A net decrease of the  $\delta^{13}\text{C}_{\text{org}}$  values initiated from the late *oxynotum* Zone or the early *raricostatum* Zone and culminating in  
a marked negative excursion of the  $\delta^{13}\text{C}_{\text{org}}$  near the Sinemurian/Pliensbachian boundary is clearly observed in the two sites.  
The amplitude of the decrease reaches -1‰ (-25 to -26‰) in the Paris Basin and -3‰ (-25 to -28‰) in the Cardigan Bay  
Basin, confirming the negative shift, highlighted by Storm et al. (2020). The condensation or even a significant hiatus in the  
northern part of the Paris Basin at the Sinemurian/Pliensbachian partly shortens this excursion and is therefore likely  
425 responsible for the difference in the amplitude of the negative excursion recorded in the two sites (Bougeault et al., 2017;  
Mercuzot et al., 2019). This decrease is equally recorded in the Sancerre Borehole in the southern Paris Basin (Fig. 1) from  
the early *raricostatum* Zone and shows an amplitude of -4 ‰ (Peti et al., 2017). The environmental significance of this  
pronounced shift can be addressed as it seems to correspond to a longer episode than the SPBE centered on the boundary or  
even beginning in the early Pliensbachian (*jamesoni* Zone) and estimated with a duration of 2 Myr on the basis of  
430 cyclostratigraphical analyses performed on the Mochras core (Ruhl et al., 2016). The stratigraphical evolution of the  $\delta^{13}\text{C}_{\text{org}}$   
could be due to changes in the type of organic matter (Suan et al., 2015). However, no change is observed in the type of organic  
matter of the Upper Sinemurian deposits of Mochras according to van de Schootbrugge et al. (2005) that highlight a dominant  
continental type. Similar conclusions arise from the study of organic matter preserved in the Montcornet borehole (Disnar et  
al., 1996). As this organic carbon trend is well recorded both in the bulk organic matter ( $\delta^{13}\text{C}_{\text{org}}$ ) resulting of a mixture of  
435 continental and marine components and in the macrofossil wood (Storm et al., 2020), the best explanation would be a  
progressive and long term input of  $^{12}\text{C}$  in both atmospheric and ocean reservoirs, that could be triggered by the volcanic activity  
and hydrothermalism linked to the CAMP, notably through the opening of the Hispanic Corridor (Price et al., 2016, Ruhl et  
al., 2016).

While this negative carbon excursion from the *raricostatum* Zone is well recorded in the  $\delta^{13}\text{C}_{\text{carb}}$  signal in the Montcornet  
440 borehole, it is surprisingly not visible in the carbonate record at Mochras, where a negative shift is recorded later at the  
beginning of the Pliensbachian and recognised as corresponding to the Sinemurian Pliensbachian Boundary Event (SPBE,  
Ruhl et al., 2016). The discrepancy between the two isotopic signals in the Mochras Borehole could be due to local diagenetic  
effect that overprint the primary signal of carbonates, as is probably also the case for the *oxynotum* Zone. Thus, the onset of  
the negative trend at the Sinemurian/Pliensbachian transition is from the early *raricostatum* Zone, while the shift reaches a  
445 maximum during the *jamesoni* Zone (plateau of low  $\delta^{13}\text{C}_{\text{org}}$  values, Storm et al., 2020) resulting from a long and progressive  
increase of light carbon release in relation with volcanism activity. Some authors (Mercuzot et al., 2019; Schöllhorn et al.,



2020a, b) previously mentioned such differences in the onset and record of the SPBE recognised in various basins worldwide which may express local diagenetic and environmental effects. This may explain why the runoff conditions, supported in this study by the kaolinite content, are firstly decreasing (i.e. *raricostatum* Zone) before drastically increasing during the *jamesoni* Zone (Deconinck et al., 2019) which should correspond to the maximal disturbance in the carbon cycle concomitant to warmer temperatures and enhanced precipitation.

## 6 Conclusions

The study of the clay mineralogy at a high resolution in the Upper Sinemurian of the Mochras and Montcornet boreholes shows that the clay minerals are mainly detrital and come from the erosion of the basement and the soil cover of the Palaeozoic massifs. The thick and continuous succession penetrated by the Mochras borehole shows significant fluctuations in the relative proportions of clay minerals. The stratigraphical succession shows an inverse relationship between the proportions of kaolinite and smectite, which probably results from an alternation of warm and humid periods with semi-arid periods. This climatic mode previously identified in the overlying Pliensbachian therefore seems to be in place at least from the Late Sinemurian. The end of the *obtusum* Zone and the *oxynotum* Zone correspond to a particularly hot and humid period favourable to a strong runoff at the origin of significant terrigenous inputs probably responsible for a repression of carbonate sedimentation. This particular hot and humid interval is also expressed by the abundances of *Classopollis* and *Liasidium variable*, by a slight negative excursion of  $\delta^{13}\text{C}_{\text{org}}$  and by low values of  $\delta^{18}\text{O}$ . However, although the low values of  $\delta^{18}\text{O}$  are consistent with high temperatures, they may also result from a decreasing salinity of seawater due to increased supplies of fresh water and/or a likely local diagenetic influence.

In the Montcornet borehole, to the north of the Paris Basin, the thinner succession has many hiatuses, notably that of the *oxynotum* Zone. The clay minerals are similar to those identified in the Cardigan Bay Basin, but the discontinuous series does not allow the alternation of humid and semi-arid periods to be identified. It is possible that this also results from the different and more distant origin of clays. In this borehole, a smectite-rich interval is identified within the *obtusum* Zone during a period of lowstand of sea level. This smectite interval, like those identified in the overlying Pliensbachian, would result from the emergence of the London-Brabant Massif then subjected to active pedogenesis. A eustatic control of the clay sedimentation is therefore expressed along the London-Brabant Massif, a situation previously proposed for the Pliensbachian, and which lasted until the end of the Jurassic.

Unlike the clay diagenesis, which is negligible, carbonate diagenesis notably expressed as nodulisation causes a dispersion of the isotopic values of  $\delta^{13}\text{C}_{\text{carb}}$ , as well as  $\delta^{18}\text{O}_{\text{carb}}$  whose interpretation in terms of palaeotemperature is unsound. The evolution of  $\delta^{13}\text{C}_{\text{org}}$  reveals a progressive decrease during the *raricostatum* Zone before the very low values at the Sinemurian/Pliensbachian transition corresponding to the SPBE.



**Acknowledgments:** The authors warmly thank J.L. Dommergues who determined ammonites newly collected during the description and sampling of the Montcornet borehole. We also thank Claude Aurière (Andra) for providing the cores from the A901 borehole. S.P.H and C.V.U. acknowledge funding from the UK Natural Environment Research Council (NE/N018508/1). J.B.R. publishes with the approval of the Chief Executive Officer, British Geological Survey (NERC). This is a contribution to the JET (Jurassic Earth Time) Project.

## References

- Ader, M., Javoy, M.: Diagenèse précoce en milieu sulfuré réducteur : une étude isotopique dans le Jurassique basal du Bassin parisien. *Comptes Rendus de l'Académie des Sciences-Séries IIA. Earth and Planetary Science*, 327(12), 803-809, 1998.
- Anderson, T.F.: Self-diffusion of carbon and oxygen in calcite by isotope exchange with carbon dioxide. *Journal of Geophysical Research*, 74(15), 3918-3932, <https://doi.org/10.1029/JB074i015p03918>, 1969.
- Barbarand, J., Bour I., Pagel, M., Quesnel, F., Delcambre, B., Dupuis, C., Yans, J.: Post-Paleozoic evolution of the northern Ardenne Massif constrained by apatite fission-track thermochronology and geological data. *BSGF – Earth Sciences Bulletin*, 189, <https://doi.org/10.1051/bsgf/2018015>, 2018.
- Beccaletto, L., Hanot, F., Serrano, O., Marc, S.: Overview of the subsurface structural pattern of the Paris Basin (France): Insights from the reprocessing and interpretation of regional seismic lines. *Marine and Petroleum Geology*, 28(4), 861-879, <https://doi.org/10.1016/j.marpetgeo.2010.11.006>, 2011.
- Bjerrum, C. J., Surlyk, F., Callomon, J. H., Slingerland, R. L.: Numerical paleoceanographic study of the Early Jurassic Transcontinental Lurasian Seaway, *Paleoceanography*, 16, 390–404, <https://doi.org/10.1029/2000PA000512>, 2001.
- Blaise, T., Barbarand, J., Kars, M., Ploquin, F., Aubourg, C., Brigaud, B., Cathelineau, M., El Albani, A., Gautheron, C., Izart, A., Janots, D., Michels, R., Pagel, M., Pozzi, J.P., Boiron, M.C., Landrein, P.: Reconstruction of low temperature (< 100° C) burial in sedimentary basins: a comparison of geothermometer in the intracontinental Paris Basin. *Marine and Petroleum Geology*, 53, 71-87, <https://doi.org/10.1016/j.marpetgeo.2013.08.019>, 2014.
- Bougeault, C., Pellenard, P., Deconinck, J.F., Hesselbo, S.P., Dommergues, J.L., Bruneau, L., Cocquerez, T., Laffont, R., Huret, E., Thibault, N.: Climatic and palaeoceanographic changes during the Pliensbachian (Early Jurassic) inferred from clay mineralogy and stable isotope (CO) geochemistry (NW Europe). *Global and Planetary Change*, 149, 139-152, <https://doi.org/10.1016/j.gloplacha.2017.01.005>, 2017.
- Brittain J.M., Higgs K.T., Riding J.B.: The palynology of the Pabay Shale Formation (Lower Jurassic) of SW Raasay, northern Scotland. *Scottish Journal of Geology*, 46(1), 67-75, <https://doi.org/10.1144/0036-9276/01-391>, 2010.
- Bucefalo Palliani, R., Riding, J.B.: A palynological investigation of the Lower and lowermost Middle Jurassic strata (Sinemurian to Aalenian) from North Yorkshire, UK. *Proceedings of the Yorkshire Geological Society*, 53(1), 1-16, <https://doi.org/10.1144/pygs.53.1.1>, 2000.
- Chamley, H.: *Clay Sedimentology*. Springer Verlag, Berlin, 623 pp, 1989.





- 510 Chandler, M.A., Rind, D., Ruedy, R.: Pangean climate during the Early Jurassic: GCM simulations and the sedimentary record of paleoclimate. *Geological Society of America Bulletin*, 104(5), 543-559, [https://doi.org/10.1130/0016-7606\(1992\)104%3C0543:PCDTEJ%3E2.3.CO;2](https://doi.org/10.1130/0016-7606(1992)104%3C0543:PCDTEJ%3E2.3.CO;2), 1992.
- Coe, A.L., Hesselbo, S.P.: Discussion of Hallam (1999). “Evidence of sea-level fall in sequence stratigraphy: examples from the Jurassic”. *Geology*, 28, 95 – 96, 2000.
- 515 Copestake, P., Johnson, B.: Lower Jurassic Foraminifera from the Llanbedr (Mochras Farm) Borehole, North/Wales, UK. *Monograph of the Palaeontographical Society, London*, 167(641), 1-403, 2014.
- Corcoran, D., Clayton, G.: Interpretation of vitrinite reflectance profiles in the central Irish Sea area: Implications for the timing of organic maturation. *Journal of Petroleum Geology*, 22(3), 261-286, <https://doi.org/10.1111/j.1747-5457.1999.tb00987.x>, 1999.
- 520 Damborenea, S. E., Echevarria, J., Ros-Franch, S.: Southern Hemisphere Palaeobiogeography of Triassic-Jurassic Marine Bivalves, Springer Briefs Seaways and Landbridges: Southern Hemisphere Biogeographic Connections Through Time, [https://doi.org/10.1007/978-94-007-5098-2\\_1](https://doi.org/10.1007/978-94-007-5098-2_1), 2013.
- Danisch, J., Kabiri, L., Nutz, A., Bodin, S.: Chemostratigraphy of Late Sinemurian–Early Pliensbachian shallow-to deep-water deposits of the Central High Atlas Basin: Paleoenvironmental implications. *Journal of African Earth Sciences*, 153, 239-525 249, <https://doi.org/10.1016/j.jafrearsci.2019.03.003>, 2019.
- Davies, J.H.F.L., Marzoli, A., Bertrand, H., Youbi, N., Ernesto, M., and Schaltegger, U.: End-Triassic mass extinction started by intrusive CAMP activity. *Nature Communications*, 8, 15596, <https://doi.org/10.1038/ncomms15596>, 2017.
- Debrabant, P., Chamley, H., Deconinck, J. F., Récourt, P., Trouiller, A.: Clay sedimentology, mineralogy and chemistry of Mesozoic sediments drilled in the northern Paris Basin. *Scientific Drilling*, 3, 138-152, 1992.
- 530 Deconinck, J. F.: Identification de l'origine détritique ou diagénétique des assemblages argileux: le cas des alternances marne-calcaire du Crétacé inférieur subalpin. *Bulletin de la Société Géologique de France.*, 3(1), 139-145, <https://doi.org/10.2113/gssgfbull.III.1.139>, 1987.
- Deconinck, J. F., Debrabant P. Diagenèse des argiles dans le domaine subalpin : rôles respectifs de la lithologie, de l'enfouissement et de la surcharge tectonique. *Revue de Géologie Dynamique et de Géographie Physique*, 26(5), 321-330, 535 1985.
- Deconinck, J.F., Chamley H.: Diversity of smectite origins in Late Cretaceous sediments: example of chalks from northern France. *Clay minerals*, 30(4), 365-379, <https://doi.org/10.1180/claymin.1995.030.4.09>, 1995.
- Deconinck, J.F., Hesselbo, S.P., Pellenard, P. 2019. Climatic and sea-level control of Jurassic (Pliensbachian) clay mineral sedimentation in the Cardigan Bay Basin, Llanbedr (Mochras Farm) borehole, Wales. *Sedimentology*, 66(7), 2769-2783, 540 <https://doi.org/10.1111/sed.12610>, 2019.
- Dellisanti, F., Pini, G.A., Baudin, F.: Use of  $T_{max}$  as a thermal maturity indicator in orogenic successions and comparison with clay mineral evolution. *Clay Minerals* 45(1), 115-130, <https://doi.org/10.1180/claymin.2010.045.1.115>, 2010.



- Dera, G., Pucéat, E., Pellenard, P., Neige, P., Delsate, D., Joachimski, M.M., Reisberg, L., Martinez, M.: Water mass exchange and variations in seawater temperature in the NW Tethys during the Early Jurassic: evidence from neodymium and oxygen isotopes of fish teeth and belemnites. *Earth and Planetary Science Letters*, 286(1-2), 198-207, <https://doi.org/10.1016/j.epsl.2009.06.027>, 2009a.
- Dera, G., Pellenard, P., Neige, P., Deconinck, J.F., Pucéat, E., Dommergues, J. L.: Distribution of clay minerals in Early Jurassic Peritethyan seas: palaeoclimatic significance inferred from multiproxy comparisons. *Palaeogeography, Palaeoclimatology, Palaeoecology*, 271(1-2), 39-51, <https://doi.org/10.1016/j.palaeo.2008.09.010>, 2009b.
- 545 Dera, G., Brigaud, B., Monna, F., Laffont, R., Pucéat, E., Deconinck, J.F., Pellenard, P., Joachimski, M.M., Durllet, C.: Climatic ups and downs in a disturbed Jurassic world. *Geology*, 39(3), 215-218, <https://doi.org/10.1130/G31579.1>, 2011.
- Dera, G., Prunier, J., Smith, P.L., Haggart, J. W., Popov, E., Guzhov, A., Rogov, M., Delsate, D., Thies, D., Cuny, G., Pucéat, E., Charbonnier, G., Bayon, G.: Nd isotope constraints on ocean circulation, paleoclimate, and continental drainage during the Jurassic breakup of Pangea. *Gondwana Research*, 27(4), 1599-1615, <https://doi.org/10.1016/j.gr.2014.02.006>, 2015.
- 555 Disnar, J.R., Le Strat, P., Farjanel, G., Fikri, A.: Sédimentation de la matière organique dans le nord-est du Bassin de Paris : conséquences sur le dépôt des argilites carbonées du Toarcien inférieur (Organic matter sedimentation in the northeast of the Paris Basin: consequences on the deposition of the lower Toarcian black shales). *Chemical geology*, 131(1-4), 15-35, [https://doi.org/10.1016/0009-2541\(96\)00021-6](https://doi.org/10.1016/0009-2541(96)00021-6), 1996.
- Dobson, M.R., Whittington, R.J.: The geology of Cardigan Bay. *Proceedings of the Geologists' Association*, 98(4), 331-353, [https://doi.org/10.1016/S0016-7878\(87\)80074-3](https://doi.org/10.1016/S0016-7878(87)80074-3), 1987.
- Duarte, L.V., Comas-Rengifo, M.J., Silva, R.L., Paredes, R., Goy, A.: Carbon isotope stratigraphy and ammonite biochronostratigraphy across the Sinemurian–Pliensbachian boundary in the western Iberian margin. *Bulletin of Geosciences*, 89(4), 719-736, <https://doi.org/10.3140/bull.geosci.1476>, 2014.
- Fauconnier, D.: Jurassic palynology from a borehole in the Champagne area, France-correlation of the lower Callovian-middle Oxfordian using sequence stratigraphy. *Review of Palaeobotany and Palynology*, 87(1), 15-26, [https://doi.org/10.1016/0034-6667\(94\)00142-7](https://doi.org/10.1016/0034-6667(94)00142-7), 1995.
- Gibbs, R.J.: Clay mineral segregation in the marine environment. *Journal of Sedimentary Petrology*, 47, 237-243, <https://doi.org/10.1306/212F713A-2B24-11D7-8648000102C1865D>, 1977.
- Godet, A., Bodin, S., Adatte, T., Föllmi, K.B.: Platform-induced clay-mineral fractionation along a northern Tethyan basin-platform transect: implications for the interpretation of Early Cretaceous climate change (Late Hauterivian-Early Aptian). *Cretaceous Research*, 29(5-6), 830-847, <https://doi.org/10.1016/j.cretres.2008.05.028>, 2008.
- Gómez, J.J., Comas-Rengifo, M.J., Goy, A.: Palaeoclimatic oscillations in the Pliensbachian (Early Jurassic) of the Asturian Basin (Northern Spain). *Climate of the Past*, 12(5), 1199-1214, <https://doi.org/10.5194/cp-12-1199-2016>, 2016.
- Guillocheau, F., Robin, C., Allemand, P., Bourquin, S., Brault, N., Dromart, G., Friedenber, R., Garcia, J.P., Gaulier, J.M., Gaumet, F., Grosdoy, B., Hanot, F., Le Strat, P., Mettraux, M., Nalpas, T., Prijac, C., Rigollet, C., Serrano, O., Grandjean, G.: 575



- Meso-Cenozoic geodynamic evolution of the Paris Basin: 3D stratigraphic constraints. *Geodinamica Acta*, 13(4), 189-245, <https://doi.org/10.1080/09853111.2000.11105372>, 2000.
- Hallam, A.: Evidence of sea-level fall in sequence stratigraphy: Examples from the Jurassic. *Geology*, 27(4), 343-346, [https://doi.org/10.1130/0091-7613\(1999\)027%3C0343:EOSLFI%3E2.3.CO;2](https://doi.org/10.1130/0091-7613(1999)027%3C0343:EOSLFI%3E2.3.CO;2), 1999.
- 580 Hallam A.: Evidence of sea-level fall in sequence stratigraphy: Examples from the Jurassic: Reply. *Geology*, 28(1), 96, [https://doi.org/10.1130/0091-7613\(2000\)28%3C96:EOSFIS%3E2.0.CO;2](https://doi.org/10.1130/0091-7613(2000)28%3C96:EOSFIS%3E2.0.CO;2), 2000.
- Han G., Pr eat, A., Chamley, H., Deconinck, J.F., Mansy, J.L.: Palaeozoic clay mineral sedimentation and diagenesis in the Dinant and Avesnes basins (Belgium, France): relationships with variscan tectonism. *Sedimentary Geology*, 136(3-4), 217-238, [https://doi.org/10.1016/S0037-0738\(00\)00103-2](https://doi.org/10.1016/S0037-0738(00)00103-2), 2000.
- 585 Haq B.U.: Jurassic Sea level Variations: A Reappraisal. *GSA today*, 28(1), 4-10, <https://doi.org/10.1130/GSATG359A.1>, 2018.
- Hardenbol, J., Thierry, J., Farley, M.B., Jacquin, T., de Graciansky, P.C., Vail, P.R.: Mesozoic and Cenozoic sequence chronostratigraphic framework of European basins. *Mesozoic and Cenozoic Sequence Stratigraphy of European Basins*. SEPM Special Publication, 60, 1998.
- 590 Hesselbo, S.P.: Sequence stratigraphy and inferred relative sea-level change from the onshore British Jurassic. *Proceedings of the Geologists' Association*, 119(1), 19-34, [https://doi.org/10.1016/S0016-7878\(59\)80069-9](https://doi.org/10.1016/S0016-7878(59)80069-9), 2008.
- Hesselbo, S.P., Bjerrum, C.J., Hinnov, L.A., MacNiocail, C., Miller, K.G., Riding, J.B., van de Schootbrugge, B. and the Mochras Revisited Science Team. Mochras borehole revisited: a new global standard for Early Jurassic earth history. *Scientific Drilling*, 16, 81–91, <https://doi.org/10.5194/sd-16-81-2013>, 2013.
- 595 Hesselbo, S.P., Deconinck, J.F., Huggett, J.M., Morgans-Bell, H.S.: Late Jurassic palaeoclimatic change from clay mineralogy and gamma-ray spectrometry of the Kimmeridge Clay, Dorset, UK. *Journal of the Geological Society*, 166(6), 1123-1133, <https://doi.org/10.1144/0016-76492009-070>, 2009.
- Hesselbo, S.P., Hudson, A.J.L., Huggett, J.M., Leng, M.J., Riding, J.B., Ullmann, C.V.: Palynological, geochemical, and mineralogical characteristics of the Early Jurassic Liasidium Event in the Cleveland Basin, Yorkshire, UK. *Newsletters on Stratigraphy*, 53, 191–211, <https://doi.org/10.1127/nos/2019/0536>, 2020.
- 600 Hesselbo, S.P., Meister, C., Gr ocke, D.R.: A potential global stratotype for the Sinemurian–Pliensbachian boundary (lower Jurassic), Robin Hood's Bay, UK: ammonite faunas and isotope stratigraphy. *Geological Magazine*, 137(6), 601–607, 2000.
- Hillier, S., Wilson, M.J., Merriman, R.J.: Clay mineralogy of the Old Red Sandstone and Devonian sedimentary rocks of Wales, Scotland and England. *Clay Minerals*, 41(1), 433-471, <https://doi.org/10.1180/0009855064110203>, 2006.
- 605 Holford, S.P., Green, P.F., Turner, J.P.: Palaeothermal and compaction studies in the Mochras borehole (NW Wales) reveal early Cretaceous and Neogene exhumation and argue against regional Palaeogene uplift in the southern Irish Sea. *Journal of the Geological Society*, 162(5), 829-840, <https://doi.org/10.1144/0016-764904-118>, 2005.
- Hudson, J.D.: Stable isotopes and limestone lithification. *Journal of the Geological Society*, 133(6), 637-660, <https://doi.org/10.1144/gsjgs.133.6.0637>, 1977.



- 610 Hurst, A.: The implications of clay mineralogy to palaeoclimate and provenance during the Jurassic in NE Scotland. *Scottish Journal of Geology*, 21(2), 143-160, <https://doi.org/10.1144/sjg21020143>, 1985.
- Jacquin, T., Dardeau, G., Durlet, C., de Graciansky, P.-C., Hantzpergue, P.: The North-Sea cycle: an overview of 2nd-order transgressive/regressive facies cycles in western Europe. In: de Graciansky, P.C., Hardenbol, J., Jacquin, T., Vail, P.R., Farley, M.B. (Eds.), *Mesozoic and Cenozoic Sequence Stratigraphy of European Basins*. SEPM Special Publication, 60, 615 445–466, 1998.
- Jeans, C.V. Clay mineralogy of the Jurassic strata of the British Isles. *Clay minerals*, 41, 187-307, <https://doi.org/10.1180/0009855064110198>, 2006.
- Jeans, C.V., Mitchell, J.G., Fisher, M.J., Wray, D.S., Hall, I.R.: Age, origin and climatic signal of English Mesozoic clays based on K/Ar signatures. *Clay minerals*, 36, 515-539, <https://doi.org/10.1180/0009855013640006>, 2001.
- 620 Jenkyns, H.C., Jones, C.E., Gröcke, D.R., Hesselbo, S.P., Parkinson, D.N.: Chemostratigraphy of the Jurassic System: applications, limitations and implications for palaeoceanography. *Journal of the Geological Society*, 159(4), 351-378, <https://doi.org/10.1144/0016-764901-130>, 2002.
- Jenkyns, H.C., Weedon, G.P.: Chemostratigraphy (CaCO<sub>3</sub>, TOC, δ<sup>13</sup>Corg) of Sinemurian (Lower Jurassic) black shales from the Wessex Basin, Dorset and palaeoenvironmental implications. *Newsletters in Stratigraphy*, 46 (1), 1–21, 625 <https://doi.org/10.1127/0078-0421/2013/0029>, 2013.
- Jones, C.E., Jenkyns, H.C., Hesselbo, S.P.: Strontium isotopes in Early Jurassic seawater. *Geochimica et Cosmochimica Acta*, 58(4), 1285-1301, [https://doi.org/10.1016/0016-7037\(94\)90382-4](https://doi.org/10.1016/0016-7037(94)90382-4), 1994.
- Kemp, S.J., Merriman, R.J., Bouch, J.E.: Clay mineral reaction progress – the maturity and burial history of the Lias Group of England and Wales. *Clay Minerals*, 40, 43–61, <https://doi.org/10.1180/0009855054010154>, 2005.
- 630 Korte, C., Hesselbo, S.P.: Shallow-marine carbon- and oxygen-isotope and elemental records indicate icehouse-greenhouse cycles during the Early Jurassic. *Paleoceanography*, 26(4), PA4219, <https://doi.org/10.1029/2011PA002160>, 2011.
- Korte, C., Hesselbo, S.P., Ullmann, C.V., Dietl, G., Ruhl, M., Schweigert, G., Thibault, N.: Jurassic climate mode governed by ocean gateway. *Nature Communications*, 6(1), 1-7, <https://doi.org/10.1038/ncomms10015>, 2015.
- Korte, C., Ruhl, M., Pálffy, J., Ullmann, C.V., Hesselbo, S.P.: Chemostratigraphy across the Triassic–Jurassic boundary. In: Sial 635 A.N., Gaucher, C., Ramkumar, M., Ferreira, V.P.: *Chemostratigraphy Across Major Chronological Boundaries*, *Geophysical Monograph*, 240, The American Geophysical Union, 2019
- Lang, W.D.: The Coinstone of the Charmouth Lias. *Proceedings of the Dorset natural history and archaeological Society*, 67, 145-149, 1945.
- Lanson, B., Sakharov, B.A., Claret, F., Drits, V.A.: Diagenetic smectite-to-illite transition in clay-rich sediments: A reappraisal 640 of X-ray diffraction results using the multi-specimen method. *American Journal of Science*, 309(6), 476-516, <https://doi.org/10.2475/06.2009.03>, 2009.



- Lefrançois, A., Deconinck, J.F., Mansy, J.L., Proust, J.N. : Structure, sédimentologie et minéralogie des argiles des formations de Beaulieu et d'Hydrequant (Dévonien supérieur du Bas-Boulonnais. *Annales de la Société Géologique du Nord*, 2, 123-134, 1993.
- 645 Lehmann, M.F., Bernasconi, S.M., Barbieri, A., McKenzie, J.A.: Preservation of organic matter and alteration of its carbon and nitrogen isotope composition during simulated and in situ early sedimentary diagenesis. *Geochimica et Cosmochimica Acta*, 66(20), 3573-3584, [https://doi.org/10.1016/S0016-7037\(02\)00968-7](https://doi.org/10.1016/S0016-7037(02)00968-7), 2002.
- Levert, J. Ferry, S.: Diagenèse argileuse complexe dans le mésozoïque subalpin révélée par cartographie des proportions relatives d'argiles selon des niveaux isochrones. *Bulletin de la Société Géologique de France*, 4, 1029-1038,  
650 <https://doi.org/10.2113/gssgfbull.IV.6.1029>, 1988.
- Marshall, J.D.: Climatic and oceanographic isotopic signals from the carbonate rock record and their preservation. *Geological Magazine*, 129(2), 143-160, <https://doi.org/10.1017/S0016756800008244>, 1992.
- Marzoli, A., Renne, P. R., Piccirillo, E. M., Ernesto, M., Bellieni, G., De Min, A.: Extensive 200-million-year-old continental flood basalts of the Central Atlantic Magmatic Province. *Science*, 284(5514), 616-618,  
655 <https://doi.org/10.1126/science.284.5414.616>, 1999.
- Masetti, D., Figus, B., Jenkyns, H.C., Barattolo, F., Mattioli, E., Posenato, R.: Carbon-isotope anomalies and demise of carbonate platforms in the Sinemurian (Early Jurassic) of the Tethyan region: evidence from the Southern Alps (Northern Italy). *Geological Magazine*, 154(3), 625-650, <https://doi.org/10.1017/S0016756816000273>, 2017.
- McHone, J.G.: Non-plume magmatism and rifting during the opening of the central Atlantic Ocean. *Tectonophysics*, 316(3-4), 287-296, [https://doi.org/10.1016/S0040-1951\(99\)00260-7](https://doi.org/10.1016/S0040-1951(99)00260-7), 2000.  
660
- Mercuzot, M., Pellenard, P., Durllet, C., Bougeault, C., Meister, C., Dommergues, J.L., Thibault, N., Baudin, F., Mathieu, O., Bruneau, L., Huret, E., El Hmidi, K.: Carbon-isotope events during the Pliensbachian (Lower Jurassic) on the African and European margins of the NW Tethyan Realm. *Newsletters on Stratigraphy*, 53(1), 41-69, <https://dx.doi.org/10.1127/nos/2019/0502>, 2019.
- 665 Merriman, R.J.: Clay mineral assemblages in British Lower Palaeozoic mudrocks. *Clay Minerals* 41(1), 473-512, <https://doi.org/10.1180/0009855064110204>, 2006.
- Meyers, P.A. 1994. Preservation of elemental and isotopic source identification of sedimentary organic matter. *Chemical Geology*, 114 (3-4), 289-302, [https://doi.org/10.1016/0009-2541\(94\)90059-0](https://doi.org/10.1016/0009-2541(94)90059-0), 1994.
- Moore, D.M., Reynolds, R.C.: *X-Ray Diffraction and the Identification and Analysis of Clay Minerals*. Oxford University Press, New York, 378 pp, 1997.  
670
- Müller, A., Parting, H., Thorez, J.: Caractères sédimentologiques et minéralogiques des couches de passage du Trias au Lias sur la bordure nord-est du Bassin de Paris. *Annales de la Société géologique de Belgique*, 96, 671-707, 1973.
- Page, K.N.: The Lower Jurassic of Europe: its subdivision and correlation. *Geological Survey of Denmark and Greenland Bulletin*, 1, 23-59, <https://doi.org/10.34194/geusb.v1.4646>, 2003.



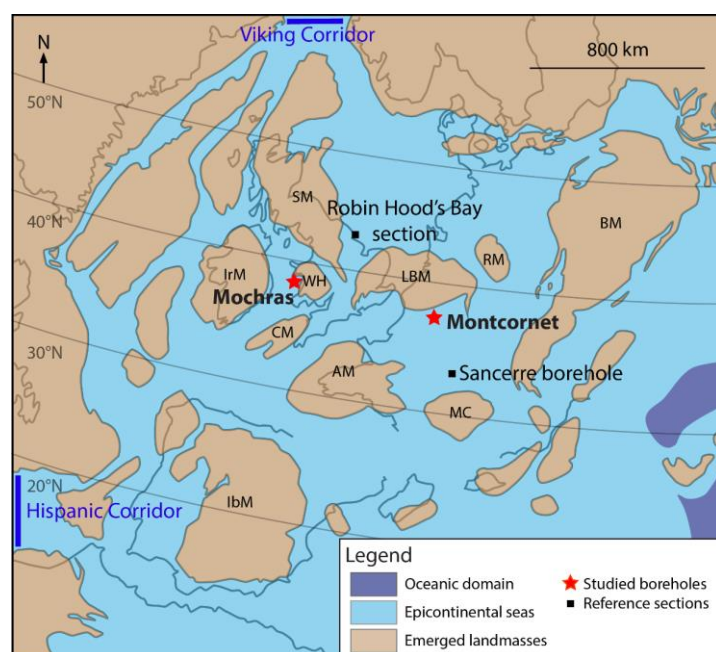
- 675 Peti, L., Thibault, N., Clémence, M. E., Korte, C., Dommergues, J. L., Bougeault, C., Pellenard, P., Jelby, M.E., Ullmann, C.V.: Sinemurian–Pliensbachian calcareous nannofossil biostratigraphy and organic carbon isotope stratigraphy in the Paris Basin: calibration to the ammonite biozonation of NW Europe. *Palaeogeography, Palaeoclimatology, Palaeoecology*, 468, 142–161, <https://doi.org/10.1016/j.palaeo.2016.12.004>, 2017.
- Petschick, R.: MacDiff 4.2.2. Available online: <http://servermac.geologie.unfrankfurt.de/Rainer.html>, 2000.
- 680 Plancq, J., Mattioli, E., Pittet, B., Baudin, F., Duarte, L.V., Boussaha, M., Grossi, V., A calcareous nannofossil and organic geochemical study of marine palaeoenvironmental changes across the Sinemurian/Pliensbachian (early Jurassic, ~191 Ma) in Portugal. *Palaeogeography, Palaeoclimatology, Palaeoecology*, 449, 1–12, <https://doi.org/10.1016/j.palaeo.2016.02.009>, 2016.
- Poças Ribeiro, N., Mendonça Filho, J.G., Duarte, L.V., Silva, R.L., Mendonça, J.O., Silva, T.F.: Palynofacies and organic  
685 geochemistry of the Sinemurian carbonate deposits in the western Lusitanian Basin (Portugal): Coimbra and Água de Madeiros formations. *International Journal of Coal Geology*, 111, 37–52, <https://doi.org/10.1016/j.coal.2012.12.006>, 2013.
- Porter, S.J., Selby, D., Suzuki, H., Gröcke, D.: Opening of a trans Pangaeian marine corridor during the Early Jurassic: insights from osmium isotopes across the Sinemurian–Pliensbachian GSSP, Robin Hood's Bay, UK. *Palaeogeography, Palaeoclimatology, Palaeoecology*, 375, 50–58, <https://doi.org/10.1016/j.palaeo.2013.02.012>, 2013.
- 690 Price, G.D., Baker, S.J., van de Velde, J., Clémence, M.E.: High-resolution carbon cycle and seawater temperature evolution during the Early Jurassic (Sinemurian–Early Pliensbachian). *Geochemistry, Geophysics, Geosystems*, 17(10), 3917–3928, <https://doi.org/10.1002/2016GC006541>, 2016.
- Riding, J.B., Leng, M.J., Kender, S., Hesselbo, S.P., Feist-Burkhardt, S.: Isotopic and palynological evidence for a new early Jurassic environmental perturbation. *Palaeogeography, Palaeoclimatology, Palaeoecology*, 374, 16–27,  
695 <https://doi.org/10.1016/j.palaeo.2012.10.019>, 2013.
- Raucsik, B., Varga, A.: Climato-environmental controls on clay mineralogy of the Hettangian–Bajocian successions of the Mecsek Mountains, Hungary: an evidence for extreme continental weathering during the early Toarcian oceanic anoxic event. *Palaeogeography, Palaeoclimatology, Palaeoecology*, 265(1–2), 1–13, <https://doi.org/10.1016/j.palaeo.2008.02.004>, 2008.
- 700 Robaszynski, F., Pomerol, B., Masure, E., Bellier, J.P., Deconinck, J.F.: Stratigraphy and stage boundaries in a type-section of the Late Cretaceous chalk from the East Paris basin: The “Craie 700” Provins boreholes. *Cretaceous Research*, 26(2), 157–169, <https://doi.org/10.1016/j.cretres.2004.10.003>, 2005.
- Ruffell, A., McKinley, J.M., Worden, R.H.: Comparison of clay mineral stratigraphy to other proxy palaeoclimate indicators in the Mesozoic of NW Europe. *Philosophical Transactions of the Royal Society of London*, 360(1793), 675–693,  
705 <https://doi.org/10.1098/rsta.2001.0961>, 2002.
- Ruhl, M., Hesselbo, S.P., Hinnov, L., Jenkyns, H. C., Xu, W., Riding J.B., Storm M., Minisini D., Ullmann C.V., Leng M.J.: Astronomical constraints on the duration of the Early Jurassic Pliensbachian Stage and global climatic fluctuations. *Earth and Planetary Science Letters*, 455, 149–165, <https://doi.org/10.1016/j.epsl.2016.08.038>, 2016.



- 710 Schöllhorn, I., Adatte, T., Van de Schootbrugge, B., Houben, A., Charbonnier, G., Janssen, N., Föllmi, K.G.: Climate and environmental response to the break-up of Pangea during the Early Jurassic (Hettangian-Pliensbachian); the Dorset coast (UK) revisited. *Global and Planetary Change*, 185, 103096, <https://doi.org/10.1016/j.gloplacha.2019.103096>, 2020a.
- Schöllhorn, I., Adatte, T., Charbonnier, G., Mattioli E., Spangenberg J.E., Föllmi, K.G.: Pliensbachian environmental perturbations and their potential link with volcanic activity: Swiss and British geochemical records. *Sedimentary Geology*, 406, 105665, <https://doi.org/10.1016/j.sedgeo.2020.105665>, 2020b.
- 715 Shaw, H.F.: Clay mineralogy of Carboniferous sandstone reservoirs, onshore and offshore UK. *Clay Minerals*, 41, 417–432, <https://doi.org/10.1180/0009855064110202>, 2006.
- Spears, D.A.: Clay mineralogy of onshore UK Carboniferous mudrocks. *Clay Minerals*, 41, 395–416, <https://doi.org/10.1180/0009855064110201>, 2006.
- Stoll, H.M., Schrag, D.P., 2000. High-resolution stable isotope records from the Upper Cretaceous rocks of Italy and Spain: Glacial episodes in a greenhouse planet? *Geological Society of America Bulletin*, 112(2), 308-319, [https://doi.org/10.1130/0016-7606\(2000\)112%3C308:HSIRFT%3E2.0.CO;2](https://doi.org/10.1130/0016-7606(2000)112%3C308:HSIRFT%3E2.0.CO;2), 2000.
- 720 Storm, M.S., Hesselbo, S.P., Jenkyns H.C., Ruhl M., Ullmann C.V., Xu W., Leng, M.J., Riding, J.B., Gorbanenko, O.: Orbital pacing and secular evolution of the Early Jurassic carbon cycle. *Proceedings of the National Academy of Sciences*, 117(8), 3974–3982, <https://doi.org/10.1073/pnas.1912094117>, 2020.
- 725 Suan, G., van de Schootbrugge, B., Adatte, T., Fiebig, J., Oschmann, W., 2015. Calibrating the magnitude of the Toarcian carbon cycle perturbation. *Paleoceanography*, 30(5), 495–509, <https://doi.org/10.1002/2014PA002758>, 2015.
- Šucha, V., Kraust, I., Gerthofferova, H., Peteš, J., Serekova, M. Smectite to illite conversion in bentonites and shales of the East Slovak Basin. *Clay Minerals*, 28(2), 243-253, <https://doi.org/10.1180/claymin.1993.028.2.06>, 1993.
- Tappin, D.R., Chadwick, R.A., Jackson, A.A., Wingfield, R.T.R., and Smith, N.J.P.: *Geology of Cardigan Bay and the Bristol Channel*. United Kingdom offshore regional report. British Geological Survey, HMSO, 107 pp, 1994.
- 730 Thierry, J. et al. (40 co-authors): Middle Toarcian. In: Dercourt, J., Gaetani, M., Vrielynck, B., Barrier, E., Biju-Duval, B., Brunet, M.-F., Cadet, J.P., Crasquin, S., Sandulescu, M. (Eds.), *Atlas Peri-Tethys Paleogeographical Maps*, vol. I-XX.CCGM/CGMW, Paris, map 8., 2000.
- Tucker R.M., Arter, G.: The tectonic evolution of the North Celtic Sea and Cardigan Bay basins with special reference to basin inversion. *Tectonophysics*, 137, 291-307, [https://doi.org/10.1016/0040-1951\(87\)90324-6](https://doi.org/10.1016/0040-1951(87)90324-6), 1987.
- 735 Ullmann, C.V., Boyle, R., Duarte, L.V., Hesselbo, S.P., Kasemann, S.A., Klein, T., Lenton, T.M., Piazza, V., Aberhan, M.: Warm afterglow from the Toarcian Oceanic Anoxic Event drives the success of deep-adapted brachiopods. *Scientific Reports*, 10(1), 1-11, <https://doi.org/10.1038/s41598-020-63487-6>, 2020
- van de Schootbrugge, B., Bailey, T.R., Rosenthal, Y., Katz, M.E., Wright, J.D., Miller, K.G., Feist-Burkhardt, S., Falkowski, P.G.: Early Jurassic climate change and the radiation of organic-walled phytoplankton in the Tethys Ocean. *Paleobiology*, 31(1), 73–97, [https://doi.org/10.1666/0094-8373\(2005\)031%3C0073:EJCCAT%3E2.0.CO;2](https://doi.org/10.1666/0094-8373(2005)031%3C0073:EJCCAT%3E2.0.CO;2), 2005.
- 740

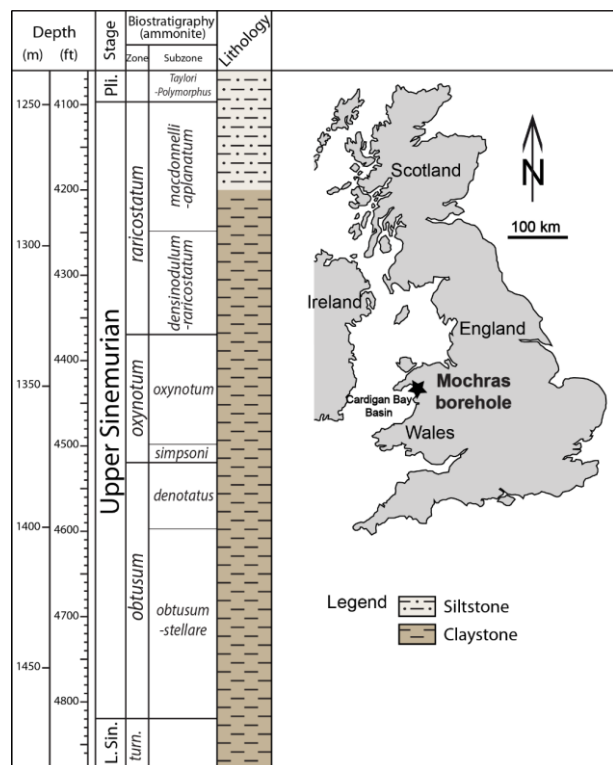


- van de Schootbrugge, B., Richoz, S., Pross, J., Luppold, F.W., Hunze, S., Wonik, T., Blau, J., Meister, C., Van der Weijst, C.M.H., Suan, G., Fraguas, A., Fiebig, J., Herrle, J.O., Guex, J., Little, C.T.S., Wignall, P.B., Püttmann, W., Oschmann, W.: The Schandelah Scientific Drilling Project: A 25-million-year record of Early Jurassic palaeo-environmental change from northern Germany. *Newsletters on Stratigraphy*, 52(3), 249-296, <https://doi.org/10.1127/nos/2018/0259>, 2019.
- 745 Wall, D.: Microplankton, pollen, and spores from the Lower Jurassic in Britain. *Micropaleontology*, 11(2), 151-190, 1965.
- Wood, A., Woodland, A.W.: Borehole at Mochras, west of Llanbedr, Merionethshire. *Nature*, 219(5161), 1352, <https://doi.org/10.1038/2191352a0>, 1968.
- Woodland, A.W. (Ed.): The Llanbedr (Mochras Farm) Borehole. Institute of Geological Sciences. Report No. 71/18, 115 pp, 750 1971.
- Xu, W., Ruhl, M., Jenkyns, H.C., Leng, M.J., Huggett, J.M., Minisini, J.M., Ullmann, C.V., Riding, J.B., Weijers, J.W.H., Storm, M.S., Hesselbo, S.P.: Evolution of the Toarcian (Early Jurassic) carbon-cycle and global climatic controls on local sedimentary processes (Cardigan Bay Basin, UK), *Earth and Planetary Science Letters*, 484, 396-411, <https://doi.org/10.1016/j.epsl.2017.12.037>, 2018.
- 755 Yang, Z., Moreau, M.G., Bucher, H., Dommergues, J.L., and Trouiller, A.: Hettangian and Sinemurian magnetostratigraphy from Paris Basin. *Journal of Geophysical Research* 101(B4), 8025-8042, <https://doi.org/10.1029/95JB03717>, 1996.



760 **Figure 1: Upper Sinemurian palaeogeographical map of the northwest Tethyan domain and position of the studied boreholes (modified from Bougeault et al., 2017). Abbreviations: SM = Scottish Massif; IrM = Irish Massif; CM = Cornubian Massif; WH = Welsh High; LBM = London-Brabant Massif; RM = Rhenish Massif; BM = Bohemian Massif; MC = Massif Central; AM = Armorican Massif; IbM = Iberian Massif.**





765 **Figure 2:** Location map of the Mochras borehole, simplified lithology and biostratigraphy of the Upper Sinemurian (from Copestake and Johnson, 2014). Abbreviations: L.Sin. = Lower Sinemurian, Pli. = Pliensbachian, turn. = turneri.

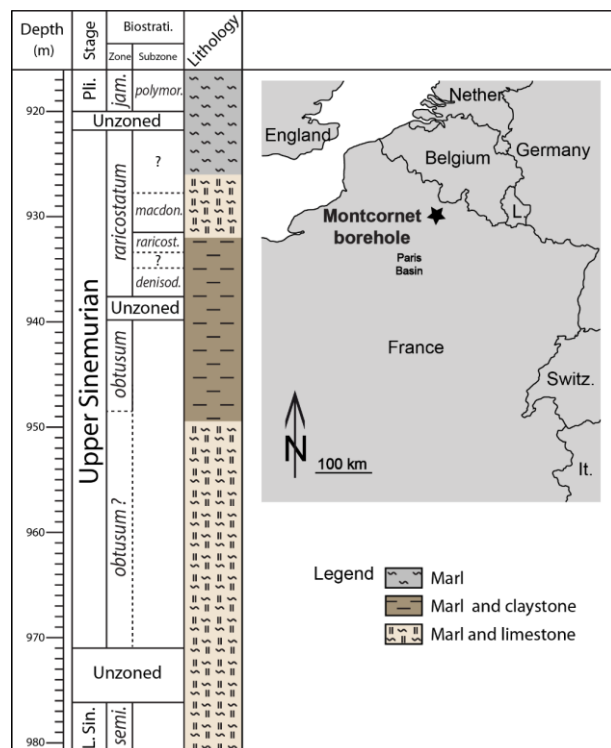


**Figure 3: Location map of Montcornet borehole, simplified lithology and biostratigraphy of Upper Sinemurian (from Fauconnier, 1995; Yang et al., 1996). *densinod.* = *densinodulum.*, *jam.* = *jamesoni*, L.Sin = Lower Sinemurian, *macdonn.* = *macdonnelli*, Pli. = Pliensbachian, *polymor.* = *polymorphus*, *raricost.* = *raricostatum*, *semi.* = *semicostatum*.**

770

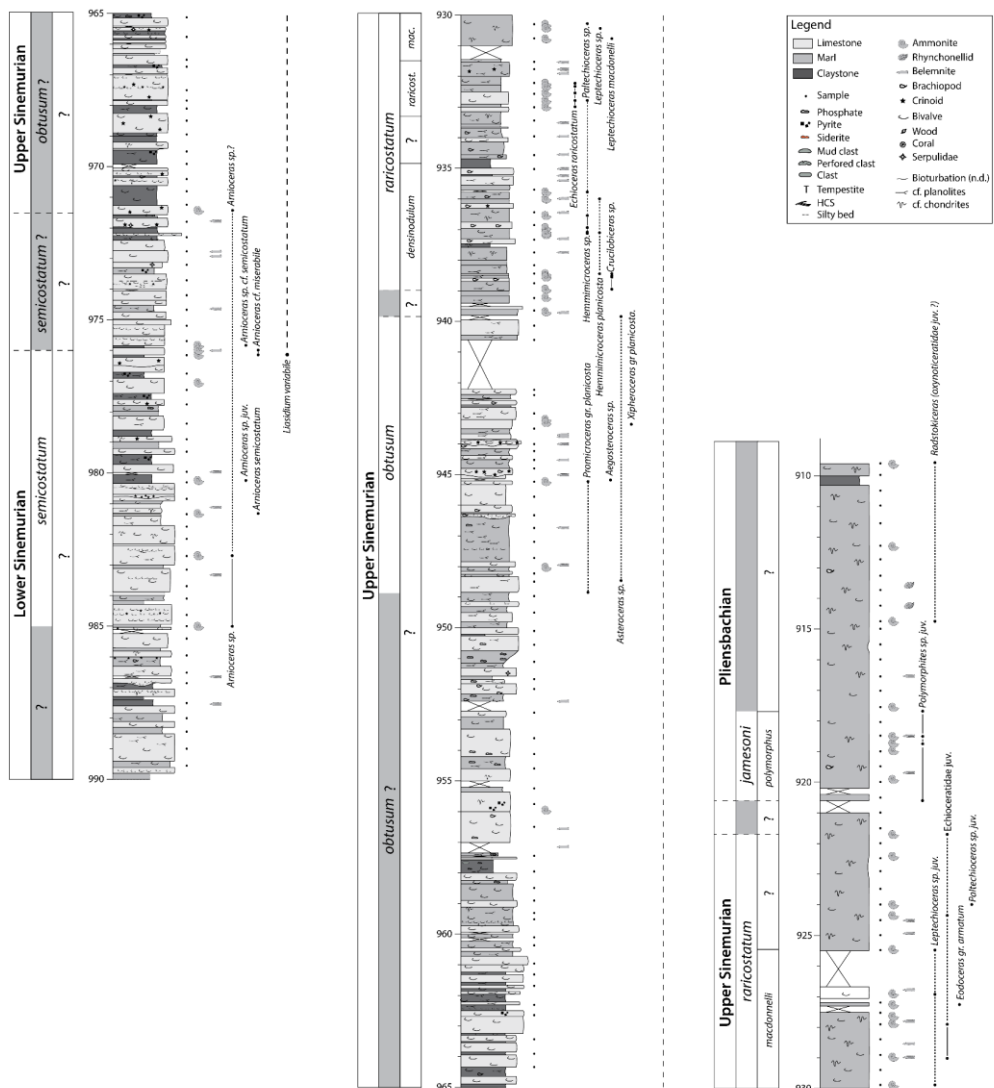
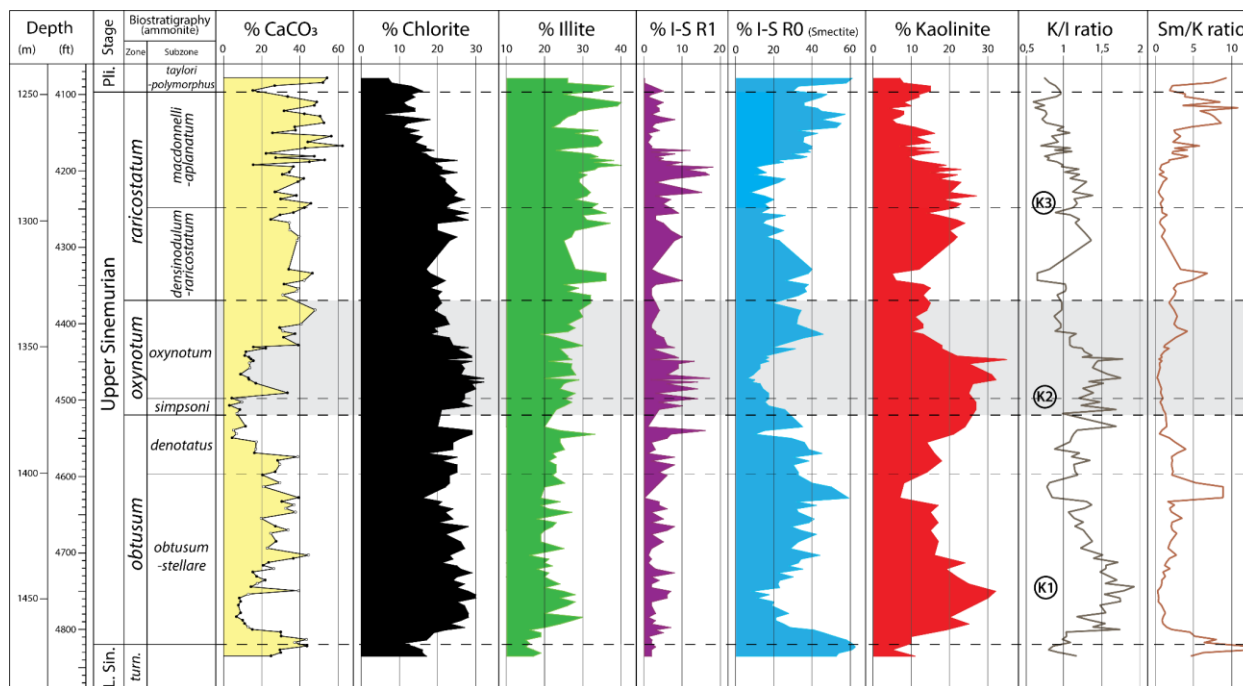
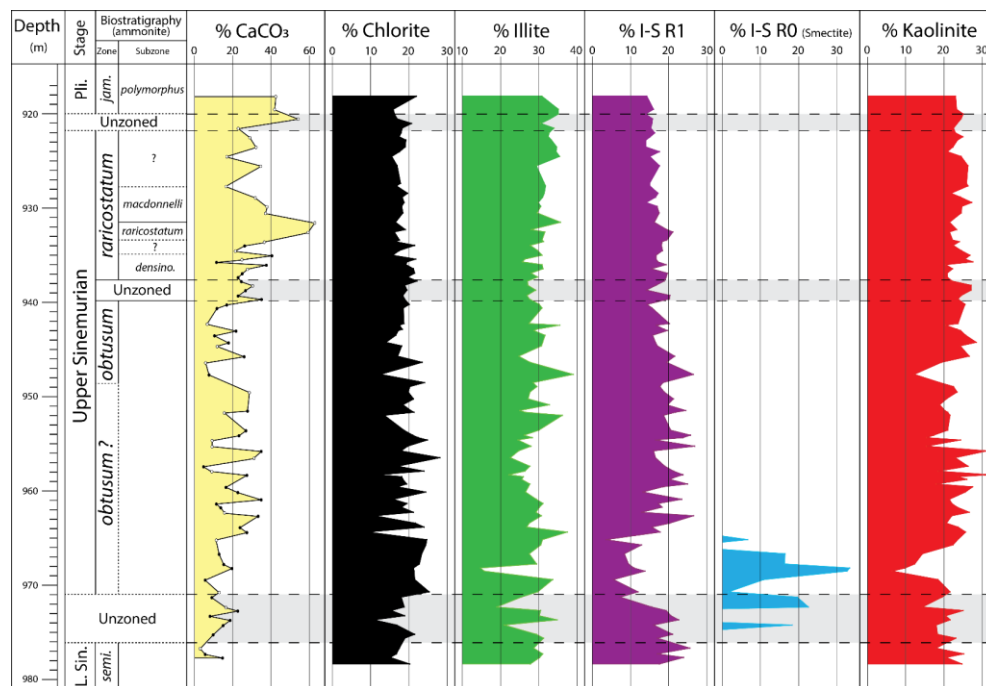


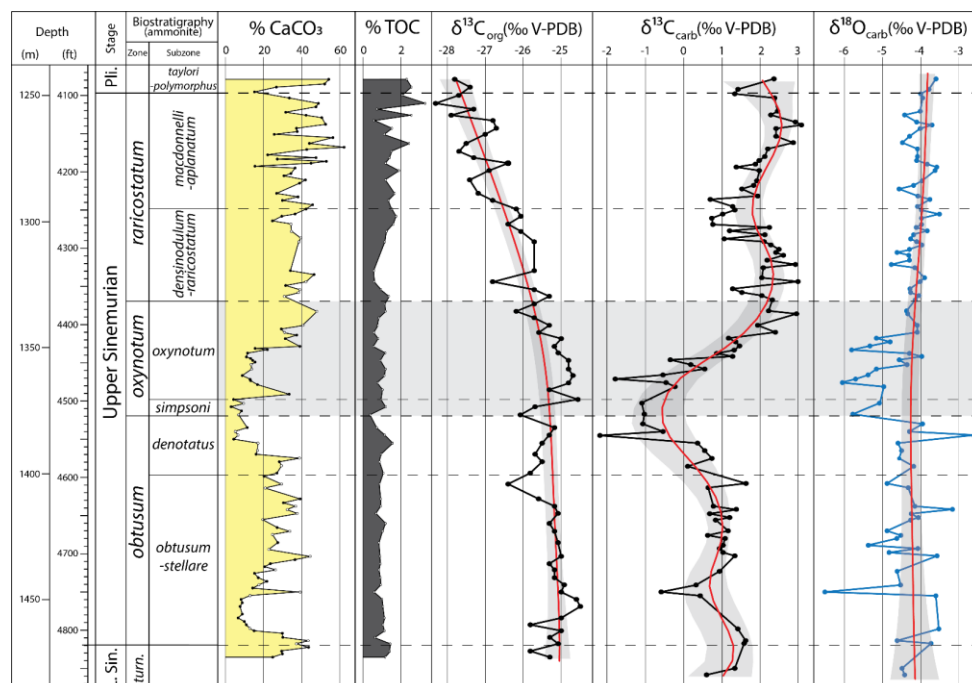
**Figure 4: Detailed lithology, sampling and biostratigraphy of Upper Sinemurian of the Montcornet borehole. Biostratigraphy modified from Yang et al. (1996) and Fauconnier (1995). Gr. – Group, juv. – Juvenile, mac. = macdonnelli, semico. = semicostatum.**



780 **Figure 5:** Calcite proportions and composition of the clay fraction of Upper Sinemurian strata of the Mochras borehole. Kaolinite/illite (K/I) and smectite/kaolinite (Sm/K) ratios corresponds to the ratio of the areas of the main peaks of these minerals. L.Sin. – Lower Sinemurian, Pli. – Pliensbachian, *turn.* = *turneri*.

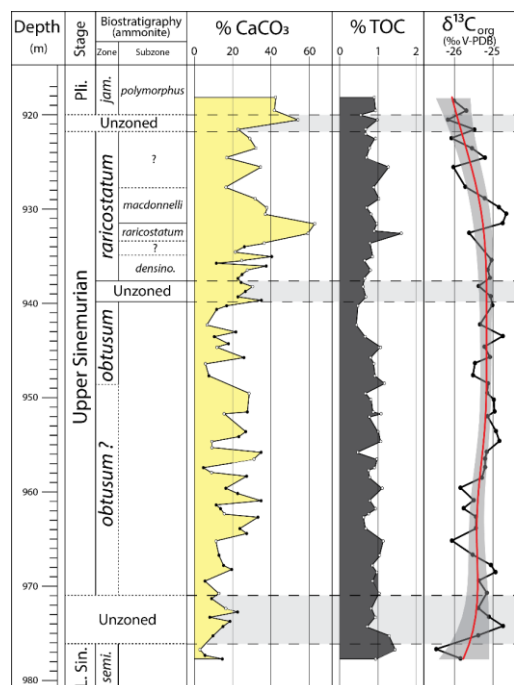


785 **Figure 6:** Calcite proportions and composition of the clay fraction of Upper Sinemurian strata of the Montcornet borehole. *densinod.* = *densinodulum*, *macdonn.* = *macdonnelli*, *Pli.* = *Pliensbachian*, *polymor.* = *polymorphus*, *raricost.* = *raricostatum*.

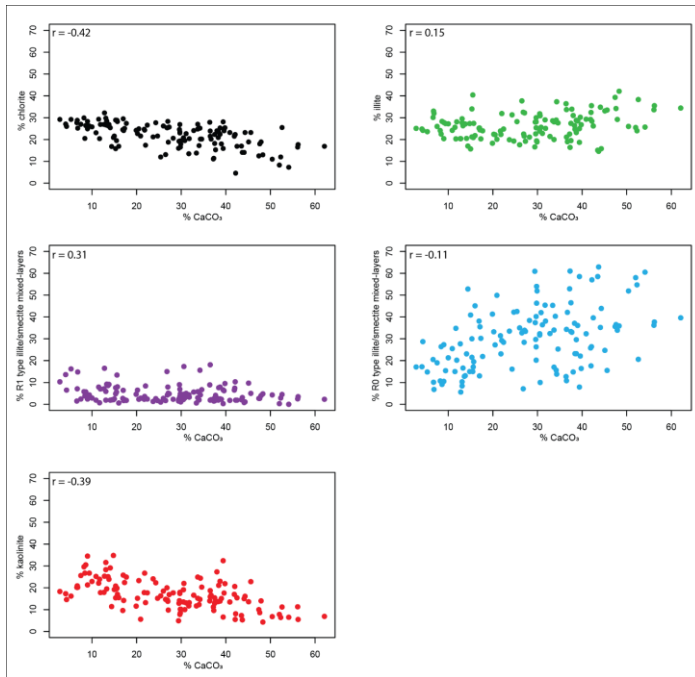




790 **Figure 7: Carbon ( $\delta^{13}\text{C}_{\text{carb}}$  and  $\delta^{13}\text{C}_{\text{org}}$ ) and oxygen ( $\delta^{18}\text{O}_{\text{carb}}$ ) isotopes of the Upper Sinemurian on the Mochras borehole coupled with the proportions of  $\text{CaCO}_3$  and TOC. Smoothing curve in red and 95% confidence interval in grey (Kernel regression). L.Sin. = Lower Sinemurian, Pli. = Pliensbachian, *turn.* = *turneri*.**



795 **Figure 8: Carbon isotopic ratio ( $\delta^{13}\text{C}_{\text{org}}$ ) of Upper Sinemurian strata of the Montcornet borehole coupled to  $\text{CaCO}_3$  and TOC proportions. Smoothing curve in red and 95% confidence interval in grey (Kernel regression). *densinod.* = *densinodulum*, L.Sin. = Lower Sinemurian, *macdonn.* = *macdonnelli*, Pli. = Pliensbachian, *polymor.* = *polymorphus*, *raricost.* = *raricostatum*, *semi.* = *semicostatum*.**



800 **Figure 9: Correlations between CaCO<sub>3</sub> content and the clay mineral relative proportions in the clay fraction in the Mochras borehole.**

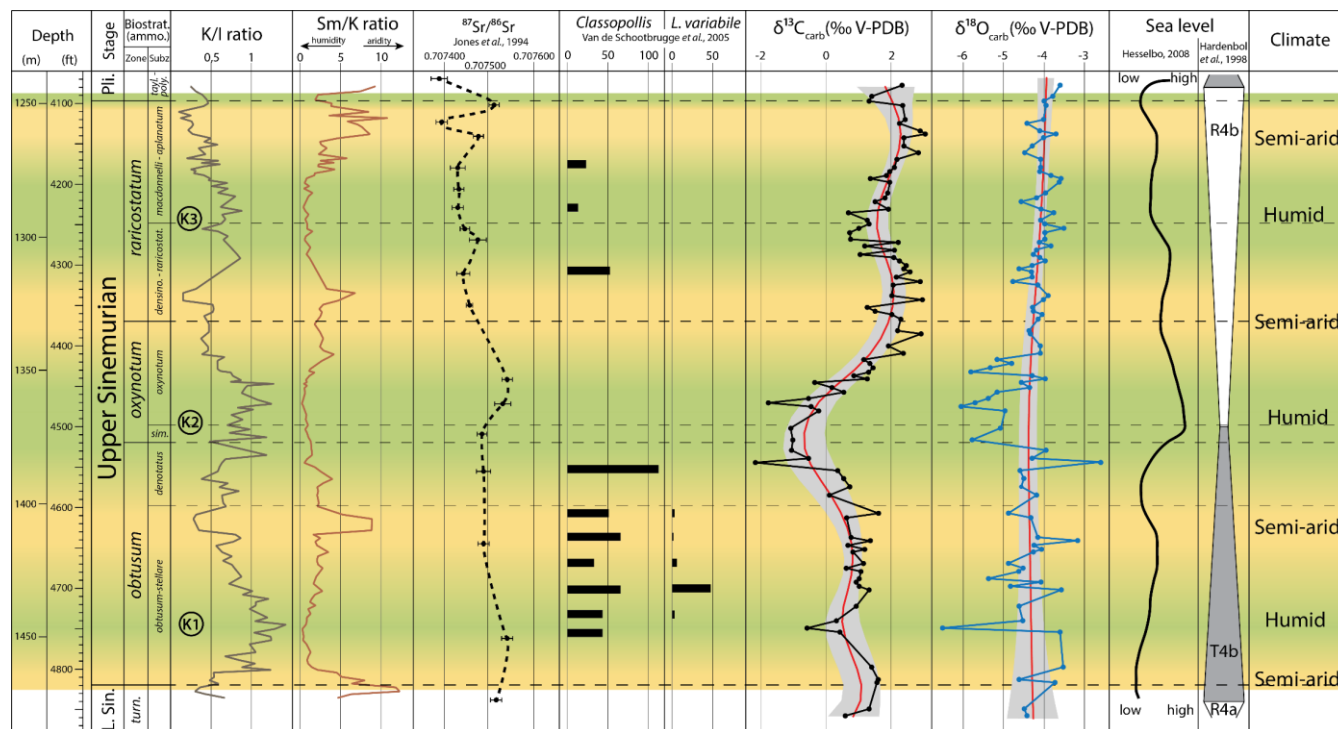


**Figure 10: Palaeoclimatic interpretations inferred from clay mineral assemblages expressed by K/I and Sm/K ratios, compared with *Classopollis*, *Liasidium variabile* abundance and strontium isotopes (Jones et al., 1994; van de Schootbrugge et al., 2005; Riding et al., 2013), carbon and oxygen isotopes variations. Eustatic variations from Hardenbol et al. (1998) and Hesselbo (2008).**

805